However, the rejection of Claims 33-42, 44, and 47-55 under 35 U.S.C. § 112, first paragraph, has been maintained. This rejection contains several sub-parts, each of which are addressed in turn below.

First, the terms "first major surface" and "opposite major surface" have been deemed new matter. It is noted that this criticism also relates to Claims 33, 35, 47 and 49.

This portion of the rejection was addressed in the paragraph bridging pages 7 and 8 of the Rule 111 Amendment. In sum, it was noted that a float glass installation in accordance with the present claimed invention produces a glass ribbon which would include a first major surface and an opposite major surface. This is the bottom and top surfaces of the glass ribbon. Indeed, the attached article by Sieger (*Chemical Characteristics of Float Glass Surfaces*, Journal of Non-Crystalline Solids 19 (1975), 213-220) refers to top and bottom surfaces of float glass. Accordingly, Applicants respectfully submit that these terms do not introduce new matter into the application and withdrawal of this portion of the rejection is requested.

Next, Claim 33 has again been criticized as introducing new matter with respect to the phrase "tin diffused therein." It is indicated that the same issue applies to Claims 35, 47 and 49.

However, as one of ordinary skill in the art would appreciate, when forming a glass ribbon on a tin bath in a float glass installation, there will necessarily be an amount of tin that is diffused into the glass ribbon at the surface in contact with the tin bath. As evidence of the same, Applicant attaches hereto, copies of three articles. These articles are the above-mentioned article by Sieger, as well as *Penetration of Tin the Bottom Surface of Float Glass : Synthesis*, Colombin *et al.*, Journal of Non-Crystalline Solids, Volumes 38 and 39, pages 551-556 (1980); and *Tin oxidation state, depth profiles of* Sn^{2+} *and* Sn^{4+} *and oxygen diffusivity in float glass by*

Mossbauer spectroscopy, Williams *et al.*, Journal of Non-Crystalline Solids, Volume 211, pages 164-172, (1997).

These articles confirm that the glass float ribbon in contact with the molten tin (sometimes referred to as the "tin side") has tin diffused in the surface which provides the tin side with a pattern of tin absorption that is different from the opposing surface which is not in contact with the molten tin (sometimes referred as the "air side"). In this regard, *see* also U.S. Patent No. 6,027,766, column 6, line 52 through column 7, line 11, which recognizes that tin diffuses into the surface of the glass float ribbon in contact with the molten tin. A copy of the '766 Patent has previously been made of record in the present application.

In view of the foregoing, Applicants respectfully submit that it clear that the diffusion of tin into the presently claimed glass float ribbon would inherently occur and thus, the phrase "tin diffused therein" does not introduce new matter.

Next, Claims 33, 35, 41, 47, 49, 51 and 55 have again been criticized as introducing new matter with respect to the term "in the crystalline phrase."

However, the evidence which has been made of record in this application clearly demonstrates that titanium dioxide deposited and annealed in accordance, for example, with Example 1 of the present application, would result in titanium dioxide in the crystalline phrase. Specifically, as discussed in paragraph 8 of Dr. McCurdy's Rule 132 Declaration submitted with the above-mentioned Rule 111 Amendment, the crystallinity of the titanium oxide coating on the glass samples prepared in accordance with Example 1 of the present application, was analyzed using X-ray diffraction. The crystallinity was confirmed as evidenced by Attachments A and B to Dr. McCurdy's Declarartion which are X-ray diffraction patterns for the samples. The X-ray

diffraction patterns show a peak at the anatase region and therefore confirmed crystallinity of the coating prepared in accordance with Example 1 of the present Application.[1]

As noted by the Examiner in the Office Action (*see*, page 5), samples were prepared in accordance with Example 1 of the present application and the two samples prepared were identical with the exception of minor variations in reflection due to processing variations. It is not possible to produce samples with exactly the same characteristics because the apparatus and processes invariably cause minor changes that would not affect the outcome of the results. Further, as discussed in paragraph 7 of Dr. McCurdy's Declaration, the line speed was decreased to 100 inches per minutes to obtain the sample having a relatively thick coating of titanium dioxide on the float glass substrate. The reason for this change was to confirm the crystallinity of the titanium oxide coating deposited on the float glass. Namely, a thicker coating is sometimes needed to conduct the X-ray diffraction analysis discussed in paragraph 8.

Thus, in sum, Applicant has faithfully reproduced Example 1 of the present application. Minor variations which do not affect the analysis being conducted invariably occur due to factors that are outside the control of the operators. The line speed was decreased in order to obtain a sample having a relatively thick coating of titanium dioxide on the float substrate. This was done in order to confirm that the deposited titanium dioxide was in fact crystalline. Example 1 of the present application does not mention that the titanium dioxide is crystalline, as noted by the Examiner in the middle of page 5 of the Office Action. However, Applicant respectfully submits that that misses the point. Applicant concedes that Example 1 does not expressly state

[1] The crystallinity of anatase titanium dioxide is well known. See, the below discussion of the book, *Physics of Thin Films*.

that the deposited titanium dioxide is crystalline. However, Applicant has demonstrated that the titanium dioxide coating deposited in accordance with Example 1 is in fact crystalline. Applicant reproduced the example in a correct manner and confirmed that the deposited material is crystalline. Accordingly, Applicant respectfully submits that the phrase "in the crystalline phase" is not new matter.

Next, Claims 33, 35, 37, 40-43, 47, 49, 51, 54 and 55 have been criticized as introducing new matter with respect to the term "photocatalytically-activated self-cleaning coating."

However, Dr. McCurdy's Declaration contains a detailed explanation of experiments which were conducted to confirm the photocatalytic activity of samples prepared in accordance with Example 1 of the present application, as well as the sample having a relatively thick titanium oxide coating prepared, as discussed above, to confirm that the titanium dioxide coating has a crystalline structure. The photocatalytic activity of these samples was confirmed using fourier transform infrared spectroscopy.

Specifically, samples were spin coated with stearic acid in methanol solution. All of the samples were referenced against untreated (*i.e.*, clean) titania coated glass. The maximum absorption at certain wavelengths was recorded and the samples were irradiated. The rate of destruction of the stearic acid film was quantified and is presented in Tables 1 and 2 of Dr. McCurdy's Declaration. This is an appropriate test to define photocatalytic activity. Stearic acid is a low volatility model organic molecule similar in chemical structure to common organic contaminants that can be found in oils and dirt. Under UV exposure, the titania will absorb the UV light and generate active surface species which then oxidize and destroy the organic contaminates on the surface of the glass, and in the process regenerate a clean titania surface for

further catalysis. The fact that this complex compound (stearic acid) can be destroyed and removed from the titania glass surface under UV exposure demonstrates the "self-cleaning" attributes of the titania glass coating of the present invention.

Again, for the reasons discussed above, Applicant acknowledges that the two samples prepared in accordance with Example 1 of the present application were identical with minor exceptions in reflection due to processing variations which would not affect the results of the data. The line speed was then intentionally changed (decreased) to 100 inches per minute to obtain a separate sample having a relatively thick coating of titanium dioxide on the float glass substrate. This was done in order to obtain a sample which could then be analyzed for purposes of crystallinity, but did not affect the quality of the data obtained.

Further, it is known that anatase titania is photocatalytic. *See*, U.S. Patent No. 6,027,766, column 3, lines 32-28, where it states "A preferred PASC coating 24 is a titanium dioxide coating. Titanium dioxide exists in an amorphous form and three crystalline forms, namely the anatase, rutile and brookite crystalline forms. Anatase phase titanium dioxide, is preferred because it exhibits strong PASC activity while also possessing excellent resistance to chemical attack and excellent physical durability."

Next, the criticism of Claims 35 and 49 as introducing new matter with respect to the term "annealing the float ribbon in air" has also been maintained.

However, Figure 1 of the present application clearly discloses that a portion of the claimed invention includes annealing the glass ribbon 18 in annealing lehr 20. This is commonly done without introducing an inert atmosphere, as is the case in the present application. In other

words, Applicant does not introduce an inert gas into the annealing lehr. Accordingly, Applicant respectfully submits that this term does not introduce new matter.

Next, the rejection of Claims 37 and 51 as introducing new matter with respect to several phrases has also been maintained. These phrases include "melting glass batch materials in a furnace," "delivering the molten glass into a bath of molten tin," "pulling the molten glass across the tin bath whereupon the glass is sized and controllably cooled," "to form a dimensionally stable glass float ribbon," "moving the float ribbon by conveying roller through a lehr," and "moving the float ribbon to a cutting station on conveying rolls where the ribbon is cut into glass sheets."

However, all of the criticized language relates to conventional aspects of float glass processess. The float glass process is discussed in the Sieger article attached hereto, and is a well known conventional process started by Pilkington in about 1960. The present invention utilizes this well known float glass process. Applicant respectfully submits that the language which has been criticized in this portion of the rejection does not introduce new matter into the specification. As discussed in the Background of the Invention section of the present application, the invention described in the present Application relates to and utilizes the well known float glass process.

To the extent there may be any possible ambiguity with respect to the phrase "dimensionally stable," Applicants respectfully submit that this phrase simply refers to the glass float ribbon having dimensions (thickness and width) which are stable as a result of a ribbon cooling into a sheet of glass that would then be cut into plates of glass.

Next, Claims 39, 41, 46, 53 and 55 have again been criticized as introducing new matter with respect to limitation of a coating thickness "up to 1300A."

However, Applicants amended each of Claims 39, 41, 46, 53 and 55 to recite a coating thickness of 1300A. There is clear support in Example 5 of Table 1 of the present application for a coating thickness of 1300A. Example 5 discloses a coating thickness of 1300A. Accordingly, withdrawal of this portion of the rejection is requested.

Claim 42 has again been criticized with respect to the phrase "said silica layer inhibits migration of sodium ions . . . self-cleaning coating." It is asserted that this phrase introduces new matter.

It is well known, however, that a silica layer would inherently inhibit migration of sodium ions. This is confirmed by U.S. Patent No. 6,265,076 (*see*, column 3, line 29). In addition, attached hereto is a portion of the book "*Physics of Thin Films*" in which it is confirmed that silica layers prevent sodium ion diffusion. See, page 109 where it is indicated that a 200 Angstrom thick silica film is already sufficient to prevent, even at high temperatures, most alkali ions at the glass surface from migrating into a subsequently deposited titanium dioxide film. Continuing, it is concluded that the appearance of the various crystal phases in the titanium dioxide fim on soda glasses can be controlled by means of a predeposited silicon dioxide layer and the the heating rate. The titanium dioxide coatings were about 60 nm in thickness (see, Table I, page 111). It is also described in this book how titania is anatase when deposited on such a film. Applicants respectfully submit that in view of the previously submitted evidenced as well as the attached evidence, it is clear that a silica layer would inhibit migration of sodium ions in the context of the present invention.

Next, Claim 44 has again been criticized as containing new matter with respect to the term "glass sheet."

It would be readily apparent to one of ordinary skill in the art that a continuous glass ribbon produced in accordance with the conventional float glass process is, in fact, a glass sheet. Withdrawal of this portion of the rejection is appropriate.

Lastly, with respect to this rejection, Claim 47 has again been criticized as containing new matter with respect to the phrase "said coating has a photocatalytically-activated self-cleaning reaction rate of at least about 8.1×10^{-3} to 9.1×10^{-3} cm^{-1} min^{-1}." It is further indicated that Claims 49, 51 and 55 contain new matter for the same reason.

As discussed at the bottom of page 13 of the Rule 111 Amendment, Claim 47 was amended to recite the reaction rate of the samples in accordance with Example 1 of the present application. These are the reaction rates of 8.1×10^{-3} to 9.1×10^{-3} cm^{-1} min^{-1}. This is the reaction rate calculated for the samples prepared in accordance with Example 1. While it is true that Example 1 did not expressly state the reaction rate, the physical materials produced in accordance with Example 1 exhibit those reaction rates. As such, the reaction rates themselves cannot be new matter.

In view of the foregoing, Applicants respectfully submit that the present claimed invention complies with the requirements of 35 U.S.C. § 112, first paragraph. Accordingly, withdrawal of this rejection is requested.

In addition, Claims 33-42, 44 and 47-55 have again been rejected under 35 U.S.C. § 112, second paragraph. Specifically, it is indicated that it is not clear whether the depositing step is different from the production step.

First, it is not clear what the Examiner intends to refer to when referencing the "production step". It is understood that the Examiner is referring to the claimed step of manufacturing a continuous glass float ribbon. This step of manufacturing the continuous glass level ribbon occurs by depositing the coating over the glass float ribbon produced in the manufacturing step. Accordingly, the step of manufacturing "or producing" the continuous closed glass float ribbon is necessarily different from the step of depositing a coating over one or more of the surfaces of the float ribbon.

In other words, in accordance with the embodiment of the present claimed invention recited in Claim 35, a continuous glass float ribbon is produced and the ribbon is then coated with titanium dioxide. It is submitted that no amendments are necessary because the claims recite the manufacture or production of continuous glass float ribbon having the first and opposite major surfaces and then depositing a coating over one or both of those surfaces.

In view of the foregoing, Applicants respectfully submit that the present claimed invention complies with the requirements of 35 U.S.C. § 112, first and second paragraphs. Accordingly, withdrawal of the rejections is requested.

In view of the above, reconsideration and allowance of this application are now believed to be in order, and such actions are hereby solicited. If any points remain in issue which the Examiner feels may be best resolved through a personal or telephone interview, the Examiner is kindly requested to contact the undersigned at the telephone number listed below.

The USPTO is directed and authorized to charge all required fees, except for the Issue Fee and the Publication Fee, to Deposit Account No. 19-4880. Please also credit any overpayments to said Deposit Account.

Respectfully submitted,

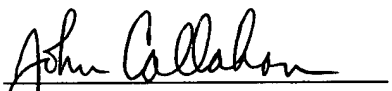

John T. Callahan
Registration No. 32,607

SUGHRUE MION, PLLC
Telephone: (202) 293-7060
Facsimile: (202) 293-7860

WASHINGTON OFFICE
23373
CUSTOMER NUMBER

Date: October 27, 2003

Journal of Non-Crystalline Solids 19 (1975) 213–220

CHEMICAL CHARACTERISTICS OF FLOAT GLASS SURFACES

John S. SIEGER
PPG Industries, Inc., Glass Research Laboratories, Pittsburgh, Pennsylvania 15238, USA

The regions near the top and bottom surfaces of float glass are chemically different from the bulk glass composition. In addition to the presence of tin oxide at the bottom surface and to a lesser extent at the top surface, differences are found in SiO_2, Na_2O, CaO, SO_3 and Fe_2O_3. The concentrations of Na_2O, CaO and SO_3 are lower at the top surface than in the bulk glass, while SiO_2 is higher. In the case of tin at the bottom surface and iron at both top and bottom surfaces, the components exist in complex concentration gradients. In addition, there are variations in oxidation state for tin, iron and sulfur. Tin appears to exist in both stannous and stannic states near the bottom surface. So far it has been found that iron at the top surface and sulfur at the bottom are largely in reduced states. Some consequences of these effects have been observed in physical and chemical behavior of the surfaces.

1. Introduction

Most modern flat glass is now produced by processes involving contact of a glass ribbon with molten tin. The change in manufacturing methods began with the advent of the Pilkington float process about 15 years ago. The products of the new methods have been suitable for most applications for which plate glass and sheet or window glass were previously used and in some respects are superior to the older products.

Investigation has shown, however, that float glass has surface chemical characteristics different in some respects from those of the bulk glass. Both surfaces of float glass have been produced under different environments than commercial glass produced by other processes. The most obvious source of difference arises from contact of one side of the production ribbon with hot tin containing varying amounts of dissolved oxygen. Other changes result from contact of the top of the ribbon with a hot reducing gas atmosphere.

2. Experimental

2.1. *Concentration profiles*

Two general methods were used to determine concentration profiles. The first, described by Sieger and Parsons [1], involved electron-microprobe analysis of the

edges of samples, either mounted in a holder or with two matching surfaces fused together. This method was useful for measurements of tin and iron profiles. Two microprobes were used: an ARL-EMX and an ARL-EMX-SM. The latter was operated typically at 15 kV and 0.02 μA sample current. For most of the tin measurements, a tin-containing soda-lime glass was used as a standard. Other details of the edge-measurement techniques are given in ref. [1].

Measurements of relative top-surface concentration profiles of SiO_2, Na_2O, CaO, SO_3 and Fe_2O_3 were made by X-ray fluorescence analysis of the glass surface as received and after etching with hydrofluoric acid. The amounts of glass removed by etching were determined by weighing or by measuring the step between an etched area and a masked area with a Talysurf 4 surface indicator (Taylor–Hobson). The surfaces of the etched samples were analyzed with a Philips PW-1212 automatic vacuum X-ray spectrometer. The HF etching procedure very probably did not produce significant preferential leaching of individual components such as Na_2O, inasmuch as etching to a depth of 20 μm or more resulted in analyses close to those of the bulk glass.

2.2. Oxidation states

2.2.1. Tin

Determination of the oxidation states of tin was made by a method described previously [1]. It involved etching off a layer from the bottom surface, complexing the fluoride, and quickly analyzing for stannous tin by titration with KIO_3 solution. Total tin was determined by reducing all tin to the stannous state with powdered nickel, cooling in a protective atmosphere and titrating with KIO_3.

2.2.2. Iron

The proportions of Fe^{2+} and Fe^{3+} were determined by a spectrophotometric method on samples ground from the top surface of the glass. The samples were dissolved in hydrofluoric acid in a protective atmosphere, and the resulting solutions were treated with boric acid, hydrochloric acid and sodium acetate. The ferrous iron was then determined by the color due to *ortho*-phenanthroline. Total iron was determined after reduction of all iron with hydroxylamine hydrochloride.

2.2.3. Sulfur

The sulfide in a bottom surface layer was determined with a specific ion electrode. A layer ground from the surface was dissolved in hydrofluoric acid and the evolved H_2S was transferred by an inert gas into NaOH solution. The latter was then titrated with $AgNO_3$ with the endpoint determined with the specific ion electrode.

3. Results and discussion

3.1. Concentration profiles

3.1.1. Tin oxide

The incorporation of tin oxide into the glass structure of the bottom of the production ribbon has been shown previously [1–3]. Typically, the concentration of tin oxide near the surface can be about 2%, with a gradient extending about 10–30 μm into the surface. Fig. 1 summarizes data previously obtained [1]. The analyses to date indicate that the depth of tin penetration found in the final product varies to some extent with glass thickness, and in all cases the amount of tin incorporated into the glass varies with the cleanliness of the tin bath. Glass near equilibrium thickness (6 mm) shows deeper tin penetration than either 3 or 12 mm. This will probably seem reasonable to most of those familiar with the float process conditions required to produce glass thinner or thicker than equilibrium.

In each case the tin penetration profile exhibits an anomalous 'hump' or satellite peak, located at about half the effective distance of tin penetration. This is probably the result of complex multicomponent diffusion effects, involving not only the tin and oxygen from the bath, but also one or more components of the glass. In addition, the tin in the glass might exhibit several valence and coordination states over the wide range of temperatures of the float bath.

The existence of a small amount of tin at the top surface has also been shown previously [1,3]. This can apparently amount to the equivalent of about 0.1% SnO_2.

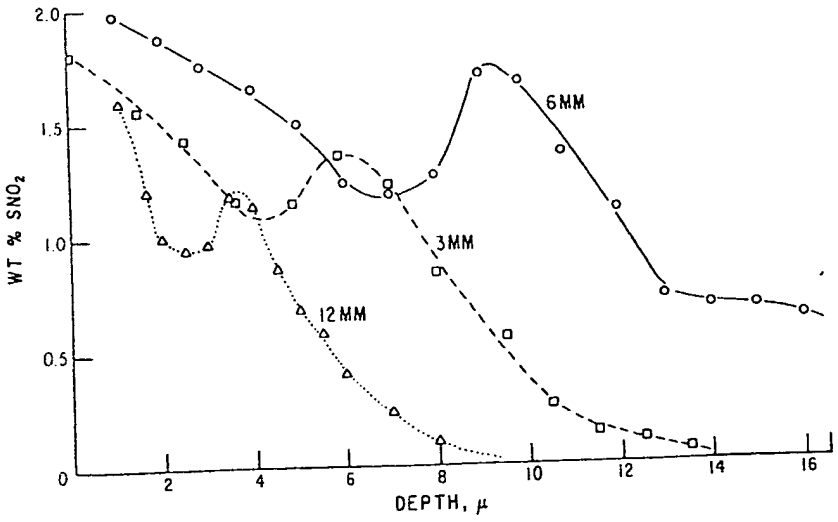

Fig. 1. Tin profiles at bottom surface of various thicknesses of clear float glass.

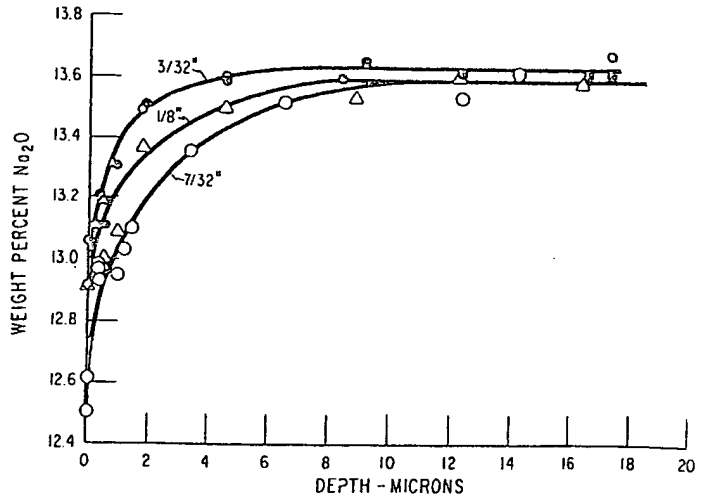

Fig. 2. Na_2O at top surface of clear float glass.

3.1.2. Principal components of the top surface

Relative concentration profiles for Na_2O, CaO, SO_3 and SiO_2 are shown in figs. 2–5, for the top surface of various thicknesses of commercial float glass. These profiles were determined by the etching and X-ray fluorescence method described previously. The X-ray fluorescence method integrates into the surface of the glass to a depth which varies with the elements determined. Without this integrating effect, the profiles would be more pronounced than shown in figs. 2–5. Since the

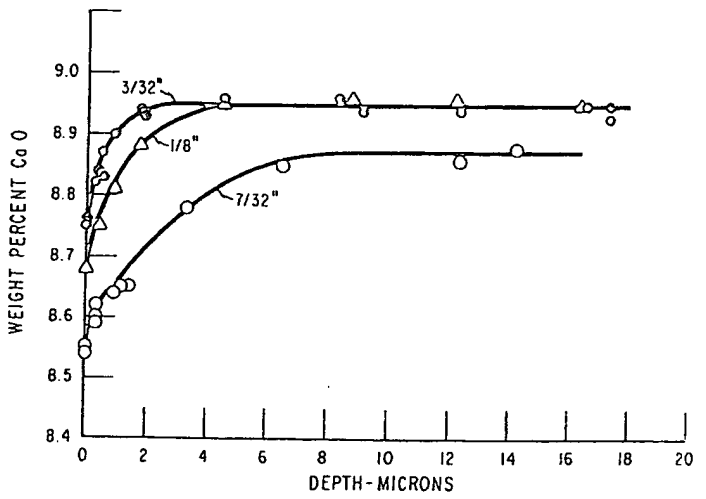

Fig. 3. CaO at top surface of clear float glass.

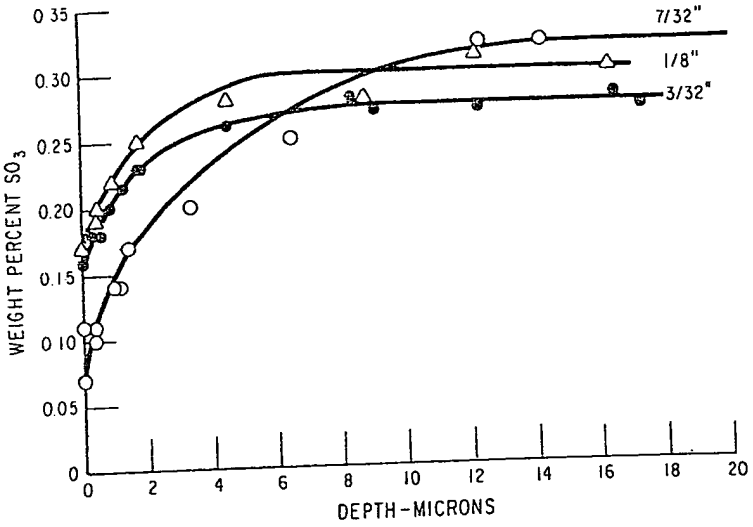

Fig. 4. SO_3 at top surface of clear float glass.

analytical totals were close to 100% in each case, there is confidence that some relative significance can be attached to the results.

As shown in the figures, SiO_2 is high at the top surface, while Na_2O, CaO and SO_3 are low. No significant concentration variation has been found for MgO. Although the data are limited, the extent of the effect apparently varies with the thickness of the glass, at least for 6 mm and thinner. Again this relative difference

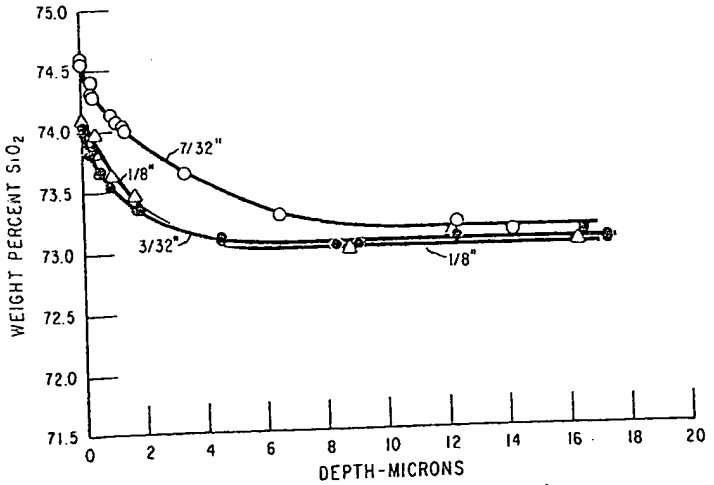

Fig. 5. SiO_2 at top surface of clear float glass.

can be rationalized in terms of the production methods used in making the thin glasses.

The low Na_2O and SO_3 at the top surface are quite probably the result of volatilization during the travel of the production ribbon down the float bath. A limited comparison with drawn pennvernon® sheet glass, made by the Pittsburgh process, shows a surface deficiency for Na_2O in this type of glass, but not as pronounced as with the top surface of float glass. Still less surface change has been found with ground and polished plate glass.

The low CaO at the top surface, found consistently in the samples analyzed, is more difficult to explain. Inasmuch as CaO is reported to raise the surface tension of glass, a low value at the surface is perhaps explainable on the basis of this property. The high concentrations of SiO_2 at the surface are probably the result of the depletion of the other constituents.

3.1.3. Iron

Concentration profiles for iron at the top and bottom surfaces of solex® float glass were determined with the electron microprobe by use of the edge-analysis procedure described previously. The results are shown in fig. 6. The measurements were actually made on samples which had been fused together as mentioned earlier; half of each curve is shown. As in the case of tin at the bottom surface, some interesting inflections are found for iron near both surfaces. The effects extend to at least 30 μm.

A qualitative check on the shape of the top surface iron profile was obtained for another sample of Solex float glass by the etching and X-ray fluorescence procedure. Fig. 7 illustrates the results. The qualitative agreement is good, in view of the integrating effect of the fluorescence method. The iron concentration is apparently low

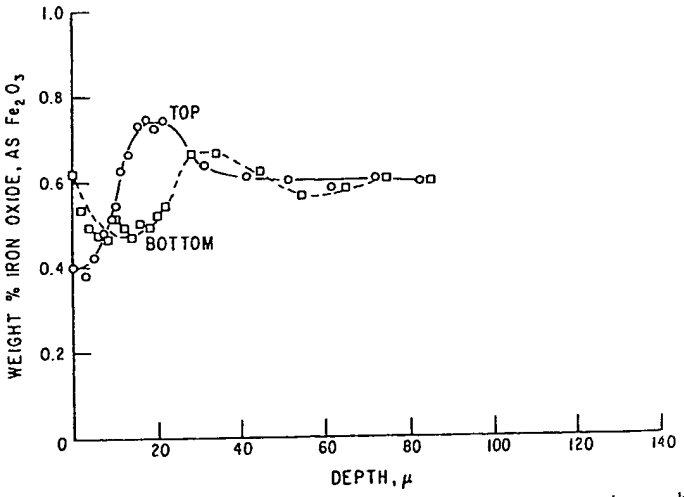

Fig. 6. Iron oxide at top and bottom surfaces of Solex float glass (electron-microprobe analysis).

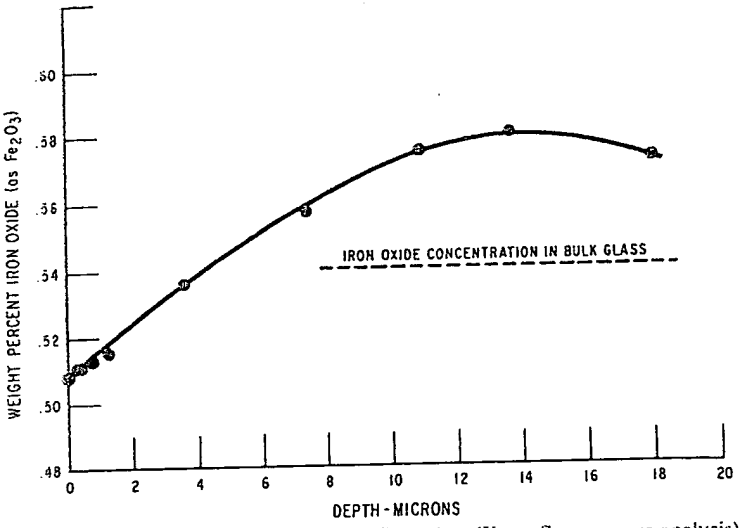

Fig. 7. Iron oxide at top surface of Solex float glass (X-ray fluorescence analysis).

near the top surface and reaches a maximum somewhat deeper in the glass, with a subsequent decline.

For the present, no attempt will be made to explain the inflections in the profiles for tin and iron. Electron microscopy has apparently ruled out phase separation, at least in the case of tin. The general phenomenon of uphill diffusion has been reported for various other systems, including glasses. Varshneya and Cooper [4] found this effect in the K_2O–SrO--SiO_2 system and related it to the theory of multicomponent diffusion. Mortlock [5] tentatively proposed surface tension as an explanation for anomalous effects in diffusion in metals. In addition, for the present cases both tin and iron can probably exist in more than one valence state and type of coordination. The observed results also reflect the result of the wide range of temperatures in a float bath. The variations in concentration are apparently real, but without a firm explanation at present.

3.2. Oxidation states

Limited results have been obtained on the oxidation states of tin, iron and sulfur in float glass. The data were obtained for tin and sulfur at the bottom surface and iron at the top surface. The presence of tin has so far interfered with measurements for iron at the bottom surface.

3.2.1. Tin

Results for tin at the bottom surface have been reported previously [1]. They indicate the presence of tin in both stannous and stannic states, with the former per-

haps predominating. Very limited measurements with Mössbauer spectroscopy on a powdered sample ground from the bottom surface seem to confirm the existence of tin in both valence states. On the other hand, a few bottom surface measurements with electron spectroscopy showed only stannic tin in the very thin outermost layer detected by this method of analysis.

3.2.2. Iron

Limited determinations were made of Fe^{2+} at the top surface of Solex float glass, containing about 0.5% iron as Fe_2O_3. The results showed that in the first 10 μm about 85% of the iron was present as Fe^{2+}. In the bulk glass only about 25% is present as Fe^{2+}. The high proportion of Fe^{2+} at the top surface is evidently the result of the reducing nature of the float-bath atmosphere.

3.2.3. Sulfur

A check was made on the presence of reduced sulfur in the first 10 μm of the bottom surface of Solex float glass. The results indicated over 30 times as much sulfide as in the bulk glass. Other data, from electron-microprobe analysis, showed a depletion in total sulfur at the bottom surface similar to the top surface. From the results it can be estimated roughly that about half of the sulfur remaining in the first 10 μm of the bottom surface is present in a reduced state. The combination of iron and reduced sulfur probably accounts for a brownish surface color that can be seen under certain critical viewing conditions.

Fortunately, the surface chemical effects in float glass very seldom lead to problems, and in some cases are of benefit. It was early recognized that too much reduced tin can lead to a 'bloom' problem in subsequent oxidizing bending and tempering applications. However, there is other evidence from cyclic humidity tests that a small amount of tin can result in improved weatherability of the bottom surface. More work remains to be done for a better understanding of some of the phenomena taking place at both top an bottom surfaces of glass produced in metal-bath processes.

Acknowledgement

The results in this paper are due in large measure to the diligent efforts of members of the Analytical Department, PPG Industries, Inc., Glass Research Center, Harmarville, Pennsylvania, USA.

References

[1] J.S. Sieger and J.M. Parsons, Tin penetration profiles in float glass, presented at the 76th Annual Meeting, Am. Ceram. Soc. (April 1974).
[2] L.A.B. Pilkington, Proc. Roy. Soc. A314 (1969) 1.
[3] R. Bruckner and J.F. Navarro, Glastech. Ber. 44 (9) (1971) 361.
[4] A.K. Varshneya and A.R. Cooper, J. Am. Ceram. Soc. 55 (6) (1972) 312.
[5] A.J. Mortlock, Trans. Met. Soc. A.I.M.E. 242 (9) (1968) 1963.

Journal of Non-Crystalline Solids 38 & 39 (1980) 551-556

PENETRATION OF TIN IN THE BOTTOM SURFACE OF FLOAT GLASS : A SYNTHESIS

L. Colombin[☆⊕], H. Charlier[⊕], A. Jelli[⊕], G. Debras[☆] and J. Verbist[☆]

☆ Facultés Universitaires de Namur, B-5000 Namur, Belgium

⊕ C.R.J., Glaverbel, B-6040 Jumet, Belgium

In the float process, tin from the float bath diffuses in the underside of the glass ribbon. It is shown that the conjugate use of several surface analysis techniques can serve to determine the full concentration profile of tin, from the first few monolayers to depths of several micrometers. Results suggest that a definite compound of sodium, tin and silicon forms in the first monolayer and that the migration process is one of diffusion accompanied by chemical reaction.

1. INTRODUCTION

In the float process, the bottom surface of the glass ribbon in the float bath remains in direct contact with molten tin for several minutes while the upper surface is exposed to a hot reducing atmosphere. In these conditions it is expectable that large variations in chemical composition, relative to that of the bulk, will occur in the superficial layers of the glass sheet.

Composition profiles in the top surface of float glass have been described in the literature [1-4] and it is known that tin diffuses in the underside to reach depths of several micrometers [4-6].

It is the purpose of this work to determine the full concentration profile of tin in the underside of float glass from the first few monolayers to depths of several micrometers. Special emphasis is attached to the first few monolayers or the first tens of nanometers since they play a most significant role in any industrial application or treatment involving the underside of float glass. No single analytical technique can provide chemical information with a sufficient resolution in depth on the first few monolayers as well as on regions situated at depths of several micrometers. One of the authors [4] has demonstrated that the conjugate use of X-ray fluorescence, Rutherford backscattering, ellipsometry, photon emission induced by ion bombardment, photoelectron spectrometry and secondary ion mass spectrometry supplies a complete and continuous range of informations on the distribution of tin from large depths to the geometrical surface of float glass.

The analysis has been carried out on one single specimen of float glass, 6.3mm in thickness, with the following chemical composition (wt %): SiO_2 72.35, Na_2O 13.86, K_2O 0.26, CaO 8.65, Fe_2O_3 0.066, Al_2O_3 0.90, SO_3 0.27 and TiO_2 0.028.

2. EXPERIMENTAL

2.1. X-ray fluorescence (XRF)

Though X-ray fluorescence is not generally considered as a surface technique, it must be emphasized that characteristic X-rays are generated in a surface layer. The thickness of this layer is large (a few micrometers) compared to that studied e.g. by photoelectron spectrometry (a few nanometers). However, this very charac-

teristic can be employed to determine long range concentration profiles, such as tin in glass, with admittedly a low resolution in depth (more than 100 nm).

A technique was developed in which the glass specimen is etched with hydrofluoric acid and in several stages to depths of a few micrometers. In between intermediate stages of etching, the characteristic fluorescence intensity of tin is recorded. The true concentration profile can be reconstructed from these intensity measurements with the help of a mathematical treatment involving an iterative sum of exponential terms and described elsewhere [4].

The actual specimen was etched in steps of 200 nm to a depth of 2000 nm, and in steps of 1000 nm to a depth of about 30000 nm. Mathematical treatment of the variation in Sn Lα intensity yields the true concentration profile which is shown graphically as a step function in figure 1.

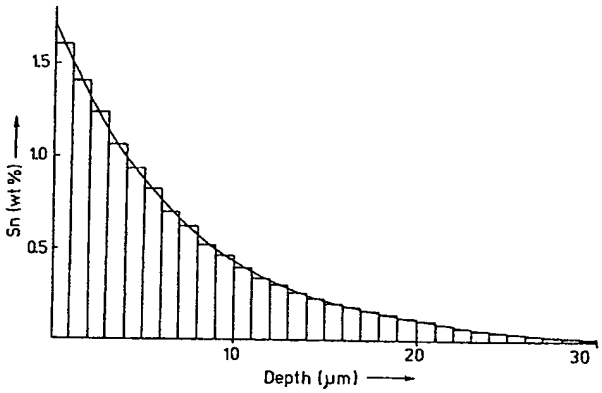

Figure 1 : X-ray fluorescence. Concentration profile of tin as a function of depth in the underside of float glass.

2.2. Rutherford backscattering

The depth resolution of XRF is insufficient to obtain much valuable chemical information on layers less than 1 micrometer in thickness. Rutherford backscattering [7] can supply such information. When a monoenergetic beam of ions strikes the surface of a specimen , some undergo elastic collisions with the nuclei of atoms occuring at, or under, the surface and are scattered. The kinetic energy of the scattered particles is related to the mass of the nucleus struck and to the depth where the elastic interaction took place. Hence, the identification and counting of atoms as well as depth information are provided by this technique.

The general energy spectrum of $^4He^+$ particles scattered by the underside of float glass is shown in figure 2. The energy of the particles is 1700 KeV, the detection angle is 135° and the detector is a surface barrier junction (300 μm), 100 mm^2 in area. The total incident charge is 4×10^{-5} C. By applying a calculation method proposed by Deconninck [7] and by using a suitable tin standard, the concentration profile of tin in the bottom side of float glass was obtained for depths comprised between 30 and 350 nm : figure 3.

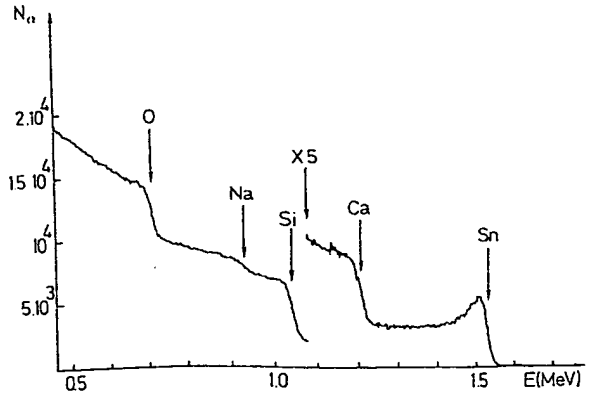

Figure 2 : Rutherford backscattering. General energy spectrum of $^4He^+$ (1700 KeV) scattered through a 135° angle by the underside of float glass.

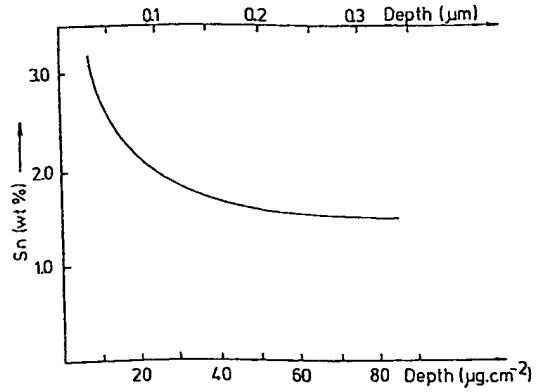

Figure 3 : Rutherford backscattering. Concentration profile of tin at intermediate depths in the underside of float glass.

2.3. Ellipsometry

Ellipsometry is a standard optical technique involving the study of the change in polarization of light upon reflection from a surface [8].

The complex refractive index n(1-ik) was determined with ellipsometry for glass surfaces (n = refractive index, k = extinction coefficient). Calculations have been carried out with the aid of a computer program [14].

Results have been published in detail elsewhere [4, 10]. They reveal that a layer, 100 nm in thickness, with abnormal optical properties occurs in the underside of float glass : the mean value of refractive index in this layer is 1.520 and the extinction coefficient is nil. By comparison, the refractive index of bulk glass is about 1.510 and the extinction coefficient is varying between 0.0070 and 0.0090.

These observations support the occurence of a thin tin-modified film, 100 nm in thickness, at the bottom surface of float glass.

2.4. Photon emission induced by ion bombardment

This technique has been extensively described by Bach [9]. During low-energy ion bombardment of a surface, atoms are sputtered in the continuum and some are in an excited state. They may relax by emission of optical photons. If the light emitted from this surface is analyzed in an optical spectrometer, emission lines are detected and allow identification of atomic species present in the specimen. As ion bombardment proceeds, further layers are removed from the surface and depth information is provided.

Tin has a major emission line at 317.5 nm. This can be located in the emission spectrum of the underside of float glass. The optical spectrometer was set on this line and the surface was bombarded by argon ions (5 KV). The tin signal which was noticeable in the initial stages of bombardment vanished rapidly with time. The etching rate was approximately 0.05 $nm.sec^{-1}$ and it was deduced from these observations that a very high concentration of tin occurs in the immediate vicinity of the surface. This concentration decreases with a steep gradient to a depth of about 10 nm where the detection limit is reached (a detailed account of this experiment has been published in [4] and [10]).

2.5. Photoelectron and secondary ion mass spectrometries

The Sn $3d_{3/2,5/2}$ doublet is easily detectable in the underside of float glass by X-ray photoelectron spectrometry. This same surface was submitted to ion bombardment (Ar^+, 1 KV) from the ion gun of a secondary ion mass spectrometer (SIMS). During bombardment tin species actually removed from the surface were observed in the SIMS spectrometer. After the removal of 10 nm of glass the photoelectron spectrum in the region of the tin doublet was again recorded. The Sn 3d peaks showed a large decrease (see [10]) in intensity which again points to the occurence of a steep concentration gradient for tin between the geometrical surface of the sheet and a depth of 10 nm. This conclusion has also been reached in more recent works by Touray [15] and Thomassin [16].

Photoelectron spectrometry can provide a more quantitative type of information. Some of the authors [2, 4] have demonstrated that, in the case of the Leybold-Heraeus spectrometer used in this work, the intensity ratios of a particular photoelectron peak to the 1s peak of oxygen can be expressed as a simple function of the number of atoms per unit volume, photoelectric cross-sections and photoelectron kinetic energies. With this method, ratios of numbers of atoms can easily be obtained from experimental data.

This technique was applied to the underside of float glass and, from the experimental observations described above, the assumption was made that the concentration profile of tin between the geometrical surface of the glass and a depth of 10 nm is expressed as a linear function of depth. It has been shown [2, 4] that this simple model can be employed to calculate ratios of numbers of atoms in the first monolayer at the bottom surface of the glass ribbon. The following values have been obtained : Sn/O 0.09, Si/O 0.30 and Sn/Si 0.30.

3. DISCUSSION AND CONCLUSION

The overall profile of tin concentration between the surface and a depth of 30 µm, as shown in figure 1, is an exponential curve of equation :

$$Sn\ (wt\ \%) = 1.83 \exp(-0.15\ x)$$

where x = depth in ångströms.10^{-4}. The tin profile obtained by Rutherford back-scattering for depths between 30 and 350 nm fits rather well to the overall curve.

According to Crank [11] this profile occurs when the mechanism of migration is one of diffusion accompanied by a first order chemical reaction freezing permanently a fraction of the diffusing substance. If the reaction rate is kC, where k is a constant and C the concentration, the balance equation is

$$\partial C / \partial t = D\, \partial^2 C / \partial t^2 - kC$$

where t is the time and D is the diffusion coefficient. In this particular case, one of the solutions of this differential equation expresses the concentration as an exponential function of distance.

However, the tin concentration exhibits a much steeper gradient in the first 10 nm under the geometrical surface of the glass sheet. Tin reaches a rather high concentration in the first monolayer : 0.09 tin atoms for 1 oxygen atom, and the question arises to determine whether this corresponds or not to a definite compound. No experimental data on the stability of tin silicates exist. Fortunately, Ghorokovskij [12] has deduced from theoretical considerations that tin silicates can only form above 1200°C while tin sodium silicates form below this temperature. As the temperature of the glass ribbon in the float bath does not exceed 1050°C, the occurence of tin silicates in the first monolayer must be rejected. However, tin sodium silicates are possible and one of them ($Na_4SnSi_3O_9$) has very much the same elemental ratios as those observed in the first monolayer of the underside of float glass : Sn/O 0.11 (glass 0.09), Si/O 0.33 (glass 0.30), Sn/Si 0.33 (glass 0.30). Though this is no definite proof of the occurence of a particular tin compound in glass it reinforces the general concept of tin migrating into the glass ribbon as the result of a diffusion accompanied by chemical reaction. Whether the permanent fixation of tin in the glass lattice and the eventual formation of stoechiometric compounds can be called crystallization or not is a controversial topic, but it can certainly be sustained that local inhomogeneities occur in the underside of float glass.

In conclusion, it remains that the migration process of tin in the bottom surface of float glass is one of diffusion with chemical reaction involving perhaps the formation of stoechiometric compounds. In the vicinity of the interface (i.e. in the first 10 or 100 nm), the concentration of tin is much higher and its gradient is very steep.

N.B. The authors want to acknowledge a recent work by Rauschenbach [13] who, by using more refined SIMS techniques, brought forward another proof of the occurence of this steep tin gradient between the surface and a depth of 10 nm.

REFERENCES

[1] Sieger, J.S., J. Non-Cryst. Solids 19 (1975) 213-220.
[2] Charlier, H., Colombin, L., Jelli, A. and Verbist, J., accepted for publication in Silicates Industriels.
[3] Chappell, R.A. and Stoddart, C.T.H., J.Mater.Sci. 12 (1977) 2001-2010.
[4] Colombin, L., "Analyse physico-chimique des zones superficielles du verre plat. Evaluation critique de diverses spectroscopies". Doctoral Thesis (1979) Facultés Universitaires de Namur, B-5000 Namur, Belgium.
[5] Sieger, J.S. and Parsons, J.M., 76th Annual Meeting, American Ceramic Society (1974).
[6] Colombin, L., Jelli, A., Charlier, H., Caudano,R., Pireaux,J.J., Riga,J.,

Tenret-Noël, C. and Verbist, J., in "Physics in Industry", eds. O'Mongain,E. and O'Toole,C.P., 113-116 (Pergamon Press, 1976).
[7] Deconninck, G. "Introduction to Radioanalytical Physics" (Elsevier, 1978)
[8] Neal, W.J. and Fane, R.W., J. Phys. E (1973) 409-416.
[9] Bach, H., Glastechn. Ber. 44 (1971) 99-109.
[10] Colombin, L., Jelli, A., Riga, J., Pireaux, J.J. and Verbist, J., J. Non-Cryst. Solids, 24 (1977) 253-258.
[11] Crank, J., "Mathematics of Diffusion" (Oxford, 1964).
[12] Ghorokovskij, V.A., Krogius, E.A., Vlasov, V.A. and Dashjevich, T.B., Izvest.Akad.Nauk S.S.S.R. Neorg.Mater., 7 (1971) 2033-2036.
[13] Rauschenbach, B. and Hinz, W., Silikattechnik, 30 (1979) 151-152.
[14] McCrackin, F.L., N.B.S. Technical Note 479 (April 1969).
[15] Touray, J.C., Scherrer, S., Champomier, F. and Naudin, F., Etude DG 5078, Compte-rendu de fin d'études DGRST, France (1978).
[16] Thomassin, J.H., Scherrer, S., Baillif, P., Touray, J.C. and Naudin, F., Bull. Minér. 102 (1979) 319-327.

ELSEVIER

Journal of Non-Crystalline Solids 211 (1997) 164–172

JOURNAL OF NON-CRYSTALLINE SOLIDS

Tin oxidation state, depth profiles of Sn^{2+} and Sn^{4+} and oxygen diffusivity in float glass by Mössbauer spectroscopy

K.F.E. Williams [a,*], C.E. Johnson [a], J. Greengrass [b], B.P. Tilley [b], D. Gelder [b], J.A. Johnson [c]

[a] *Department of Physics, University of Liverpool, PO Box 147, Liverpool L69 7ZE, UK*
[b] *Pilkington Technology Management, Lathom, Ormskirk, UK*
[c] *School of the Built Environment, Liverpool John Moores University, Liverpool, UK*

Received 5 June 1996; revised 12 August 1996

Abstract

Mössbauer transmission spectra of tin in commercially produced soda–lime–silica float glass have been obtained at low temperatures. It was found that between 20% and 37% of the tin which had diffused into the lower surface of the ribbon during manufacture was in the Sn^{4+} state. An estimate of the depth profiles for each oxidation state was obtained by measuring the Mössbauer spectra of samples after increasing thicknesses of the tin surface had been removed by polishing. These revealed that about 60% of the total Sn^{2+} occurs in the first 3.5 μm, when the total tin penetration depth was 17 μm. Heat treatments were conducted to investigate the rate of oxidation of Sn^{2+} to Sn^{4+} in the glass. The diffusivity of oxygen into the glass was estimated to vary between 1.29×10^{-18} m^2 s^{-1} at 500°C and 1.92×10^{-16} m^2 s^{-1} at 730°C. Measurements of the decrease in recoil-free fraction with temperature enabled values for the Debye temperatures Θ_D of Sn^{2+} and Sn^{4+} to be found to be 185 and 260 K respectively. These results show that the binding of tin at the surface of float glass is weaker than in bulk tin-containing glasses where Θ_D was 200 K and 319 K.

PACS: 61.40; 76.80 + y; 98.20

1. Introduction

The production of flat glass by floating it on molten tin causes a small amount of tin to be taken up into the bottom surface of the glass [1]. This tin may present a problem when the glass is heat treated during thermal toughening: a wrinkling can appear on the surface of the glass called "bloom". As this may be associated with the oxidation of the tin from Sn^{2+} to Sn^{4+} it is important to establish the oxidation state of the diffused tin. The small quantities make it difficult to determine the oxidation state of the tin by chemical methods, but Mössbauer spectroscopy has proved to be a successful technique for obtaining this information.

Tin-119 is the second most commonly studied Mössbauer isotope. Tin Mössbauer spectra measure

* Corresponding author. Tel.: +44-151 794 3423; fax: +44-151 794 3441; e-mail: kfe22@liverpool.ac.uk.

PII S0022-3093(96)00636-9

the hyperfine interactions of the ^{119}Sn nucleus with its environment. As these are sensitive to small changes in the surrounding electron density, the two oxidation states Sn^{2+} and Sn^{4+} are clearly distinguishable. Sn^{2+} having the larger shift and quadrupole splitting. Results have been obtained at temperatures of 77 K or below, because of the increase in the Mössbauer effect at low temperatures. The accuracy of the measurement of the ratio of Sn^{2+} to Sn^{4+} is also improved as the difference in the temperature dependence of the effect for the two tin states is less as the temperature approaches 0 K.

Information on the oxidation state of tin near the surface of float glass has been previously obtained at room temperature using conversion electron Mössbauer spectroscopy (CEMS) by Principi et al. [2], who showed that both Sn^{2+} and Sn^{4+} exist in float glass.

The ratio of the amount of each oxidation state has also been studied for tin in tin-doped float glass [3]. In those measurements the bulk glass contained between 3% and 15% tin oxide by weight, i.e. between 1.2 and 6.2 mol%. This provides a useful comparison with float glass since the surface of float glass may contain up to 20 mol% tin oxide. This relatively large amount of tin in the doped-float samples is measurable by chemical analysis, and the results can be compared with those deduced from Mössbauer spectra. Since the recoil-free fraction f depends upon the strength of binding which is different for the two ionic states, it was necessary to make measurements as a function of temperature in order to determine them and hence obtain accurate results on the Sn^{2+}/Sn^{4+} ratio. The results thus obtained were in very good agreement with those given by chemical analysis.

There is considerable interest in determining the depth to which tin has diffused into float glass, and especially how the Sn^{2+}/Sn^{4+} ratio changes with depth. Previous measurements of the variation of the total tin content with depth have been made by electron microprobe analysis (EMPA) [4,5] and cathodoluminescence [6]. They showed that the tin penetrated to a depth of several tens of microns, which increased with the thickness of the glass. Measurements to depths close to the surface (down to 0.5 μm) have been made by X-ray photoelectron spectroscopy (XPS), secondary ion mass spectroscopy (SIMS) and Rutherford backscattering spectroscopy (RBS) [5].

In this paper the amount of each oxidation state of tin in different specimens of float glass was determined and their depth profiles were estimated. Effects of heat treatment on the tin were made and diffusivity of oxygen was estimated.

2. Experimental details

The float glass studied had been manufactured to different thicknesses, but most samples discussed here were prepared from 6 mm thick glass. The samples were prepared from the first 0.1 mm of the lower surface of the ribbon. The region of glass above this, containing virtually no tin, was removed to increase the quality of the spectra obtained. The remaining thin layers were ground and placed in a sample holder which could be held in a cryostat at 77 K or below. In order to discover the effect on the oxidation state of the position across the float ribbon width, samples were obtained from the centre and the edge of the ribbon at two different manufacturing lines.

A further three specimens were prepared in order to measure the depth profile of Sn^{2+} and Sn^{4+} as follows: small indentations were made in discs of the glass ribbon to different depths as a means of establishing how much glass would be removed from the surface. Different weights were applied to create three indentations per disc. The discs were placed on a rotating board and secured. A silicon based spray containing small particles of diamond was used as an abrasive to polish away the glass as the board revolved. At intervals, the discs were viewed under a microscope and the depths of the remaining indentations were measured. A Mössbauer sample containing the full depth of tin was prepared and subsequent samples were prepared which had 1.5 μm, 3.5 μm and 7.5 μm successively removed from the bottom surface by the above technique. The total amount of tin in each sample was measured by X-ray fluorescence (XRF) and oxidation state ratios were established by Mössbauer spectroscopy.

The Mössbauer spectra were taken in transmission geometry at 77 K and below. A 10 mCi source of ^{119}Sn in calcium stannate $CaSnO_3$ was used. The

23.8 keV γ-ray was detected with a thin liquid nitrogen cooled intrinsic germanium crystal with a high efficiency. The resolution was 0.7 keV so that the γ-ray was easily distinguished from the 25.4 keV X-ray. The energy scale was calibrated using a ^{57}CoRh source and an α-iron absorber at room temperature. A least squares fitting program was used to analyze the spectra and yielded values of chemical shift, quadrupole splitting and intensity (area) of each component.

The tin content (i.e. quantity of tin in each specimen) was monitored by XRF. The depth of penetration of tin was measured by EMPA by scanning across a polished cross section, and XPS was used to determine the near-surface profile by repeatedly etching the surface with argon ions.

Two samples underwent a bloom test, which involves heating in air at 730°C for 10 min. Following these tests several heat treatments were carried out on samples from the same glass ribbon. They were heated for times between 30 min and 345 h at temperatures of 500, 600 and 730°C in a muffle furnace which was not under vacuum. A further heat treatment was carried out above the liquidus temperature, at 1050°C for 10–15 min; it was then quenched in water. X-ray diffraction (XRD) measurements were made to check for the possibility of crystallization.

In order to measure the binding strength of the Sn^{2+} and Sn^{4+}, spectra of the tin in one float glass sample were recorded using a variable temperature cryostat between about 10 and 300 K.

3. Results

Fig. 1 shows some typical Mössbauer spectra and it is seen that both Sn^{2+} and Sn^{4+} are present.

Table 1
XRF tin count and percentage of Sn^{4+} at the edge and centre of the float glass ribbon from two plants

Float line	Position	Tin count	Percentage Sn^{4+} ($\pm \leq 1\%$)
1	edge	1805	30.3
	centre	1380	36.6
2	edge	1223	25.5
	centre	1091	27.2

Table 2
XRF tin count and effective Sn^{2+} and Sn^{4+} contributions for sections of float glass of different depths

Region (μm)	Tin count	Calculated	
		Sn^{4+} count	Sn^{2+} count
0–17	4638	955	3683
17 less 1.5	3528	857	2671
17 less 3.5	2266	784	1482
17 less 7.5	1412	514	898

Tin counts were obtained by XRF and showed that there was a greater amount of tin present in the samples obtained from the edges than in the centre of the ribbon for both lines. The resulting Mössbauer spectra were similar for the two different ribbons and these are shown for one of the lines in Fig. 1(a, b). For both lines, the percentage of Sn^{4+} is less at the edges than at the centre and therefore less when the tin content is greater as shown in Table 1.

The samples were prepared as described above in order to study how the tin oxidation state varied with depth. Electron microprobe measurements showed that the tin extended to a depth of about 17 μm (Fig. 2). This also showed a small maximum at about 7 μm, similar to that obtained by Sieger [4].

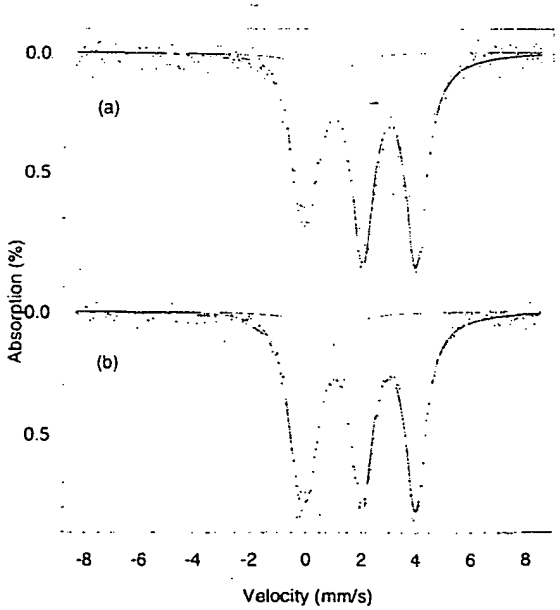

Fig. 1. Mössbauer spectra at 77 K of ^{119}Sn in float glass taken from (a) the edge and (b) the centre of the ribbon.

Table 3
Tin counts from Table 2 calculated for each region of the float glass surface and the percentage contributions of Sn^{2+} and Sn^{4+} in each region considered

Region (μm)	Tin count	Percentage Sn^{4+} ($\pm < 1\%$)	Percentage Sn^{2+} ($\pm < 1\%$)
0–17	4638	20.6	79.4
0–1.5	1110	8.8	91.2
1.5–3.5	1262	5.8	94.2
3.5–7.5	854	31.0	69.0
7.5–17	1412	36.3	63.7

The Mössbauer spectra of each of the samples, including that of the full 17 μm sample, are shown in Fig. 3 and the fractions of Sn^{2+} and Sn^{4+} deduced from them are shown in Table 2 together with the XRF data. The results obtained enabled us to calculate the fraction of the tin in each oxidation state in the regions 0–1.5 μm, 1.5–3.5 μm, 3.5–7.5 μm and 7.5–17 μm where measurements could not be made directly. These data are shown in Table 3, and the proportions of the two oxidation states in the regions considered are plotted in Fig. 4. The results show that the majority of the tin nearest the surface exists as Sn^{2+}, about 60% of which occurs in the first 3.5 μm. By contrast about 80% of Sn^{4+} is at a depth greater than 3.5 μm.

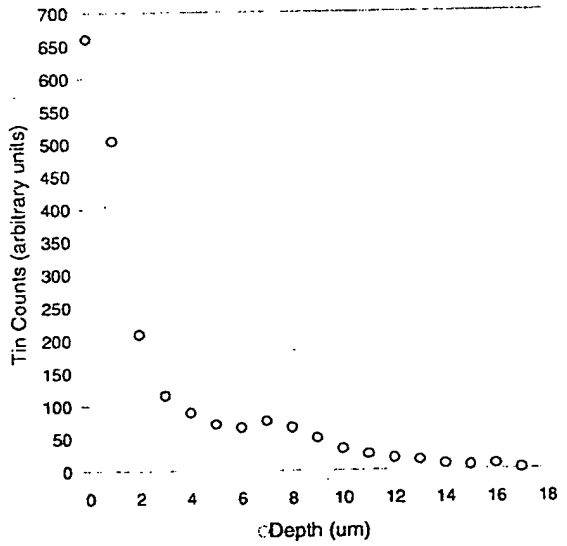

Fig. 2. Depth profile of the total tin concentration in the lower surface of the float glass sample used for oxidation state depth profile measurements obtained by EMPA.

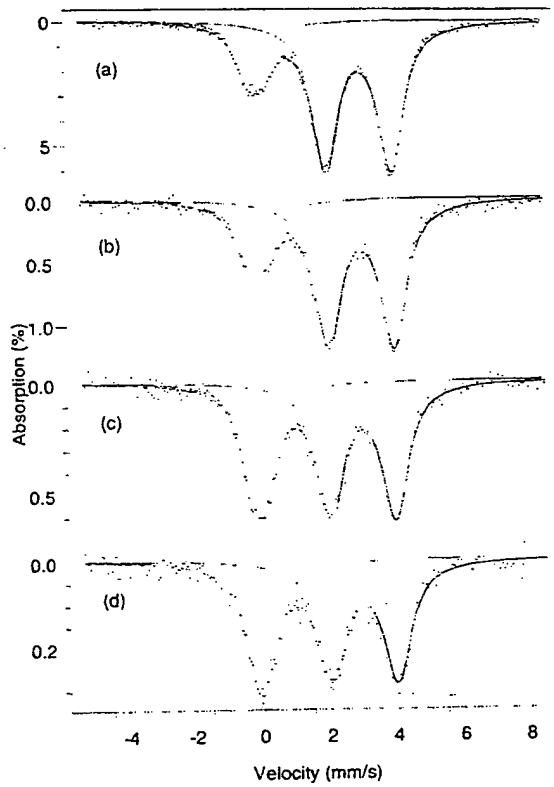

Fig. 3. Mössbauer spectra at 77 K of ^{119}Sn in (a) a float glass sample containing tin to a depth of 17 μm and of the same material with a further (b) 1.5 μm (c) 3.5 μm and (d) 7.5 μm removed from it.

The glass which had undergone the bloom test showed a typical wrinkling of the surface. The Mössbauer spectra of the glass before and after heating are shown in Fig. 5. Analysis of the spectra shows that a small amount of Sn^{2+} has been oxidised to Sn^{4+}. For sample 1 there was an increase in the amount of Sn^{4+} from 14.5% to 21.9% and in sample 2 there was an increase from 34.5% to 37.3%. Principi found a larger increase than this probably because his results were obtained from the surface only. The near-surface depth profile obtained by X-ray photoelectron spectroscopy (XPS) showed that there was some movement of the tin on heating (Fig. 6).

The XRD measurements showed that at temperatures of 500 and 600°C the specimens remained as glasses. After 193 and 338 h heating at ~ 730°C, the XRD patterns (Fig. 7) of the glass showed that

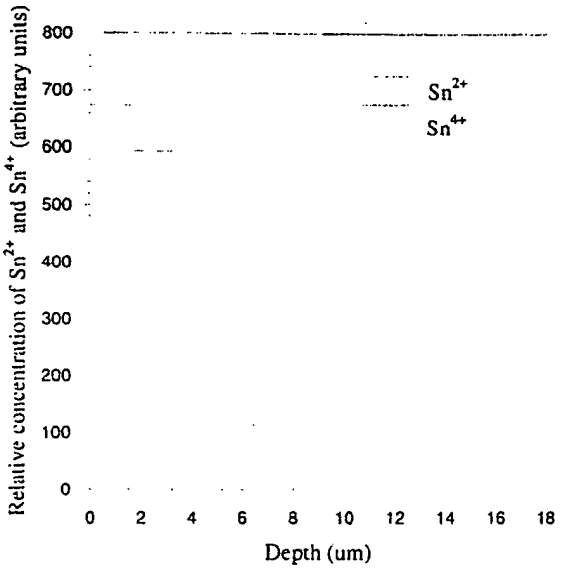

Fig. 4. Histogram showing approximate depth profiles of (a) Sn^{2+} and (b) Sn^{4+} in float glass.

devitrification had occurred and crystalline SnO_2 was present.

Mössbauer spectra were recorded at 77 K and a series of spectra for the glass heated at 730°C for

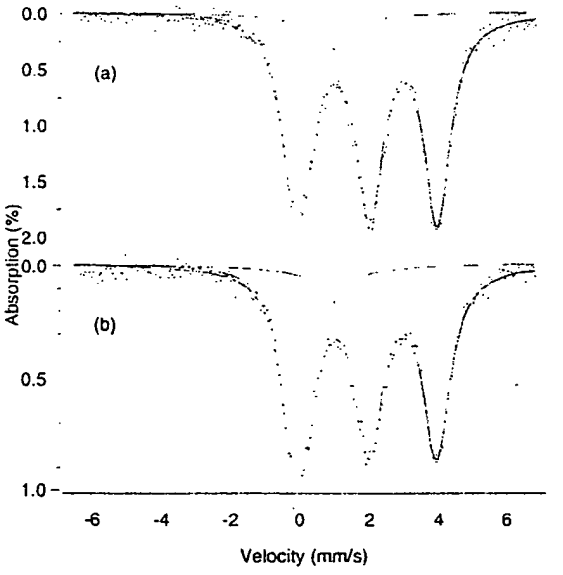

Fig. 5. Mössbauer spectra of ^{119}Sn at 77 K for a sample (a) before and (b) after a "bloom" test.

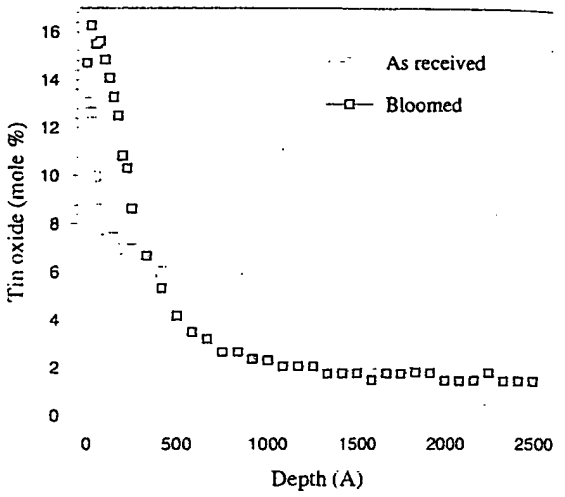

Fig. 6. Near-surface depth profiles of tin in float glass determined by XPS showing diffusion of tin during a "bloom" test.

different times is plotted in Fig. 8. This shows an increase in oxidation with increasing time. The samples heated at 500 and 600°C showed similar behaviour, with the rate of oxidation being lower at lower temperatures as expected. At 730°C some Sn^{2+} still remains even after 345 h, but above 1000°C all the Sn^{2+} was converted to Sn^{4+} within a short time.

In order to determine the rate of oxidation of Sn^{2+} the percentage of Sn^{4+} in each of the samples

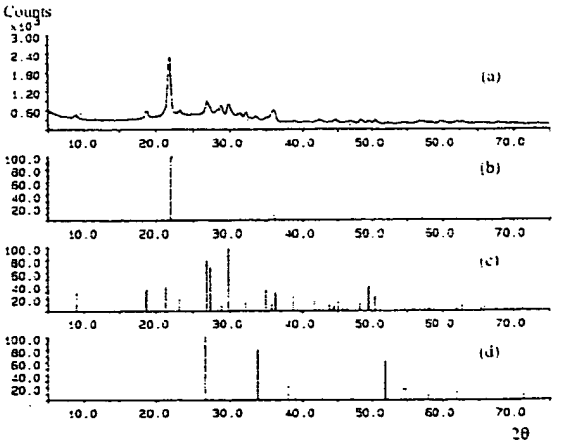

Fig. 7. (a) XRD pattern of the bottom surface of float glass after heating at 730°C for 338 h. Also shown are the patterns expected for crystalline (b), SiO_2 (c), $Na_2Ca_2SiO_6$ and (d) SnO_2.

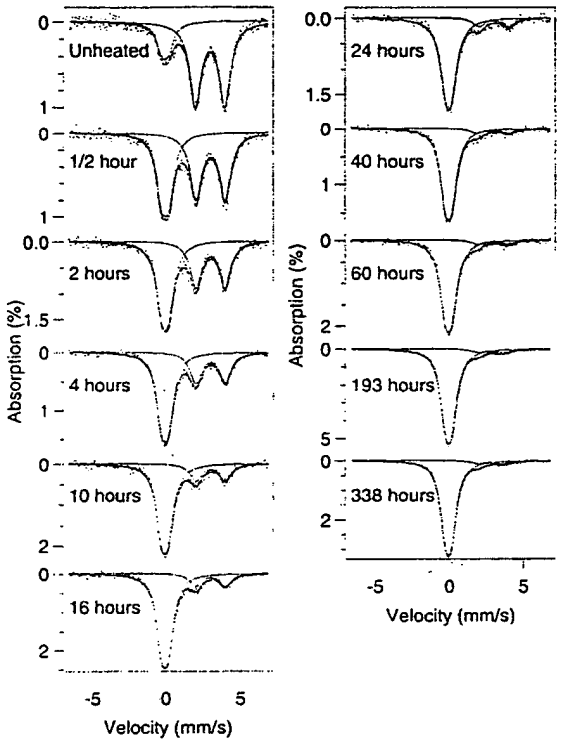

Fig. 8. Mössbauer spectra at 77 K of ^{119}Sn in float glass heated at 730°C for times up to 338 h.

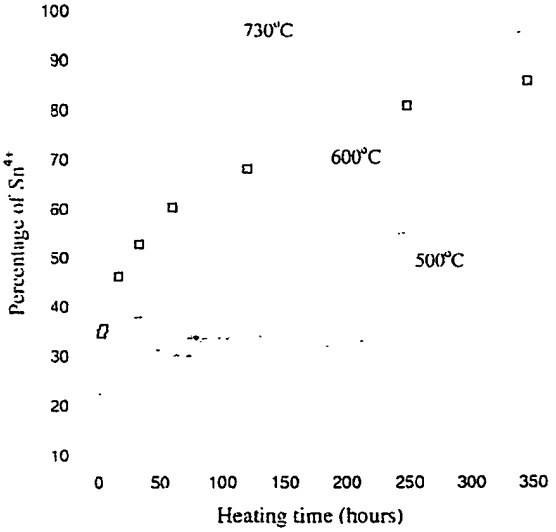

Fig. 9. Fraction of Sn^{4+} in float glass as a function of time when heated at different temperatures. The lines are fits as described in the text.

was plotted against heating time for temperatures of 500, 600 and 730°C. These data are shown in Fig. 9 together with the curves generated from a model of oxygen diffusivity and the subsequent oxidation of Sn^{2+} to Sn^{4+}.

The variation of the recoil-free fraction with temperature was used to determine the Debye temperatures of the Sn^{2+} and Sn^{4+} in the glass [3]. The changes in the ratio of the intensities, i.e. the difference of the recoil-free fraction, f, are apparent from the spectra shown in Fig. 10. The dependence of ln f versus temperature is shown in Fig. 11; it is clear

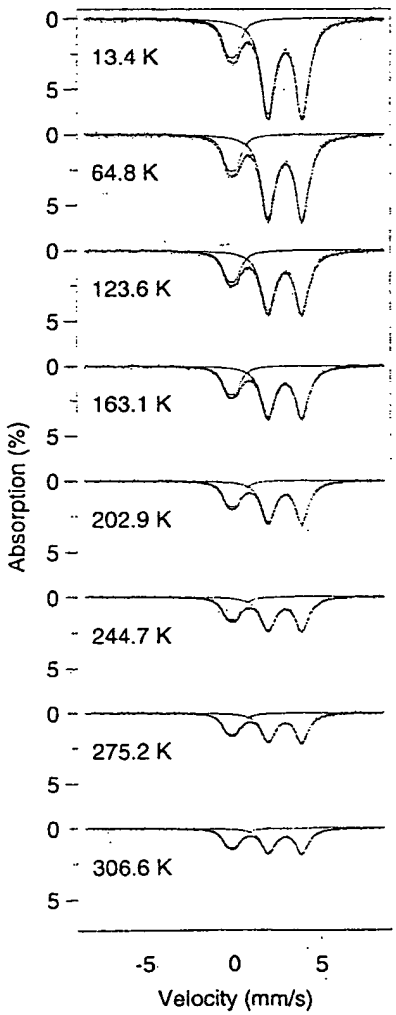

Fig. 10. Mössbauer spectra of ^{119}Sn in float glass as a function of temperature.

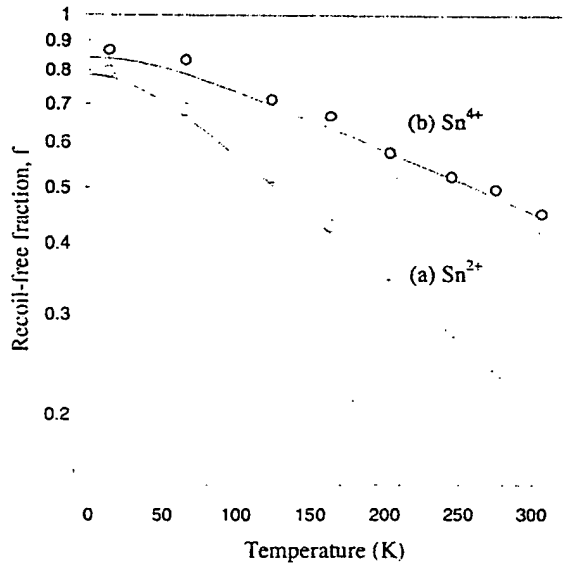

Fig. 11. Variation of $\ln f$ with temperature for (a) Sn^{2+} and (b) Sn^{4+} in float glass.

from this figure that the Sn^{2+} is less tightly bound than Sn^{4+}. Debye temperatures Θ_D were found to be 185 K for Sn^{2+} and 260 K for Sn^{4+}. These are less than those found for the corresponding component in re-melted tin-doped float glasses i.e. 200 K and 319 K for Sn^{2+} and Sn^{4+} respectively [3].

4. Discussion

The results given in Table 1 differ somewhat from those found for the specimens used by Principi et al [2]. From previous results we have consistently found that where there is a large amount of diffused tin, the relative amount of Sn^{4+} goes down. This could indicate that there may be a limit to the amount of Sn^{4+} which can be present in as-manufactured glass. A direct comparison between these results and those of Principi cannot be made because the former were done at 77 K and the latter at room temperature which leads to different f factors. In addition Principi's CEMS measurements are specific to the surface while in the transmission spectra we are looking at the total tin present.

At the edges of the ribbon a small width of tin is exposed to the bath atmosphere allowing greater amounts of oxygen to be dissolved in the tin there. This leads to the formation of tin ions (Sn^{2+}) within the molten tin at the edges of the bath. Studies by Franz [7] suggest that the presence of tin ions sets up exchange processes with other ions in the glass, such as Na^+ and Ca^{2+}, due to concentration gradients and redox reactions. Pilkington [1] has investigated the effect of oxygen being present in the tin bath, and noted that the greater the oxygen content in the tin bath the greater the amount of tin in the glass.

The results provide a rough estimate of the depth profiles for each oxidation state. Although it was not possible to determine accurately the depths removed by polishing, the distribution of tin oxidation states suggests that the maximum in the EMPA profile (around 7 μm in Fig. 2) may be associated with the increase in Sn^{4+} to Sn^{2+} tin ratio.

The uptake of tin into glass is assumed to satisfy the diffusion equation:

$$\frac{\partial c}{\partial t} = D\frac{\partial^2 c}{\partial x^2},$$

where c is the concentration at a depth x, t is the time of diffusion and D is the diffusivity. A solution of this equation is

$$c(x) = c_0\left(1 - \mathrm{erf}\frac{x}{x_0}\right),$$

where c_0 is the tin concentration at the surface and x_0 characterises the mean thickness of the tin layer and is the depth at which $c = 0.16c_0$. We assume that this distribution remains unchanged during the heat treatment in air, which is a reasonable approximation since the rate of diffusion of tin in glass is much slower than that of oxygen.

The diffusion of oxygen into the glass is also governed by the diffusion equation with D being the diffusivity for oxygen into glass, and the solution for the oxygen concentration at a depth x after heating for a time t is

$$c^{O_2}(x, t) = c_0^{O_2}\left(1 - \mathrm{erf}\frac{x}{2\sqrt{DT}}\right).$$

As the oxygen diffuses in during heating the Sn^{2+} becomes oxidized to Sn^{4+}. The probability of an Sn^{2+} ion being oxidized to Sn^{4+} is assumed to be proportional to its concentration and that of the

Table 4
Oxygen diffusivity as a function of temperature

Temperature (°C)	Oxygen diffusivity (D) ($m^2\ s^{-1}$)
500	1.285×10^{-18}
600	9.598×10^{-18}
730	1.92×10^{-16}

oxygen. If the initial concentration of Sn^{4+} is c_0^{4+} and that of Sn^{2+} is c_0^{2+}, then the amount of Sn^{4+} after a time t is

$$c^{4+}(t) = c_0^{4+} + c_0^{2+}\frac{\int_0^{\infty} c^{2+}(x)c^{O=}(x,t)\,dx}{\int_0^{\infty} c^{2+}(x)\,dx} = c_0^{4+} + c_0^{2+} \times \frac{\int_0^{\infty}(1-\mathrm{erf}(x/x_0))\left(1-\mathrm{erf}\left(x/2\sqrt{DT}\right)\right)dx}{\int_0^{\infty}(1-\mathrm{erf}(x/x_0))\,dx}.$$

The value of x_0 was estimated to be 3.5 μm from the tin profile data of the unheated glass, measured by electron microprobe analysis (EMPA) (see Fig. 2). The values $c_0^{4+}=0.2$ and $c_0^{2+}=0.8$ were taken from the spectrum of the unheated sample. This model was then used to obtain a fit to the data. The best fit was achieved by varying the value of the diffusivity, D, until the lowest possible χ^2 was produced. This provided an estimate of the oxygen diffusivity under the conditions stated. The fits are shown as the solid lines in Fig. 9, and the values of D are given in Table 4. They are of the same order of magnitude as those obtained for the diffusion of oxygen into fused silica and soda–lime–silicate glass [8].

If the diffusivity is expressed in terms of activation across an energy barrier of height Δ, i.e.

$$D = D_0 e^{-\Delta/kT},$$

then the data of Table 4 yield the values $D_0 = 3.3\times10^{-9}\ m^2 s^{-1}$ and $\Delta = 1.45$ eV.

The Debye model, although not strictly applicable to glasses, is useful in parametrizing the data to compare different samples. The fraction, f of recoil-free events is proportional to the absorption area of the spectra, and the slope of $\ln A$ or $\ln f$ versus T in the high temperature region (≥ 150 K) may be used to determine a Debye temperature for each component in the spectra [9]. Debye temperatures were evaluated for the samples which had been heat treated as described in Section 2 and are presented in Table 5 together with the corresponding isomer shift data. The results suggest that there has been little change in the strength of binding of the Sn^{2+} ions. There was also little change in Θ_D for the Sn^{4+} ions when the sample was heated to 500°C which is reasonable as this is below the glass transition temperature (about 580°C for float glass of the composition used). However, after heating at 730°C for 2 h the strength of binding of the Sn^{4+} appears to increase. The fact that this value does not increase after heating at 1050°C for 10 min followed by rapid cooling could be investigated further, particularly as all the Sn^{2+} has been converted to Sn^{4+}. Heating above T_1 would produce a more open glass matrix, and the present result may be explained because this structure could be "frozen in" on cooling rapidly, leading to a lower Debye temperature for Sn^{4+}.

The results show that the Sn^{2+} ions are acting as modifiers as found in binary glasses which were studied previously [9]. Sn^{4+} may be acting as an intermediate but could have difficulty entering the

Table 5
Effect of heating on the amounts, Debye temperatures Θ_D and isomer shifts δ of Sn^{2+} and Sn^{4+} in float glass

Float glass sample	Percentage Sn^{4+}	$\Theta_D(Sn^{4+})$ (K)	$\Theta_D(Sn^{2+})$ (K)	Sn^{4+} [a] shift (δ) ($mm\ s^{-1}$)	Sn^{2+} [a] shift (δ) ($mm\ s^{-1}$)
Unheated	20.6 ($\pm \leq 1\%$)	260($\pm$0.2)	185($\pm$0.1)	−0.203 ($\pm$0.017)	2.862 ($\pm$0.007)
120 h at 500°C	45.2 ($\pm \leq 1\%$)	258($\pm$0.4)	180($\pm$0.2)	−0.174 ($\pm$0.005)	2.862 ($\pm$0.007)
2 h at 730°C	55.3 ($\pm \leq 1\%$)	282($\pm$0.6)	187($\pm$0.4)	−0.227 ($\pm$0.068)	2.829 ($\pm$0.010)
10 min at 1050°C	100 ($\pm \leq 1\%$)	263($\pm$0.5)	—	−0.176 ($\pm$0.001)	—

[a] The isomer shifts are quoted relative to calcium stannate at 290 K.

network as much of the tin enters the ribbon after the glass network was already formed. This is unlike the situation of the re-melted tin-doped float samples where the tin is present while the network forms.

5. Conclusions

Mössbauer spectroscopy indicates that the majority of tin was Sn^{2+} and is more weakly bound than the Sn^{4+}.

More tin is taken up at the edges of the float bath than in the center due to the greater quantity of oxygen present, but the proportion of Sn^{4+} is less in this region.

Measurement of the depth profile indicated that the Sn^{2+} concentration is six or seven times that of Sn^{4+} in the first few μm, but beyond 5 μm into the glass the concentrations differ only by a factor of 2.

Heat treatment in air results in oxidation, being more apparent at higher temperatures particularly above the glass transition temperature. A theoretical diffusion model was found to give a good fit to the data and values of the diffusivity of oxygen into glass were obtained.

The measurement of the Debye temperatures showed that for both Sn^{2+} and Sn^{4+} Θ_D was lower than that of tin ions in re-melted doped float glass. This is not surprising, as in manufactured float glass the tin diffuses in over a few minutes as the ribbon passes over the molten tin, whereas in making the doped float samples the samples are heated to a much higher temperature and allowed to come to equilibrium in a crucible.

Acknowledgements

We gratefully acknowledge the help of Mr. R.A. Chappell, Mr. D.R. Oakley, Miss C. Lunt and Mr. D.J. Taylor, and useful discussions with Dr. D. Holland. KFEW acknowledges the financial support of the Engineering and Physical Sciences Research Council and Pilkington. This work was supported by the Engineering and Physical Sciences Research Council and Pilkington. The authors thank the directors of Pilkington plc and Dr. A. Ledwith, Director of Group Research, for permission to publish this paper.

References

[1] L.A.B. Pilkington, Proc. R. Soc. London A 314 (1969) 1.
[2] G. Principi, A. Maddalena, A. Gupta, F. Geotti-Bianchini, S. Hreglich and M. Verità, Nucl. Instr. Meth. Phys. Res. B 76 (1993) 215.
[3] J.A. Johnson, C.E. Johnson, K.F.E. Williams, D. Holland and M.M. Karim, Hyperfine Interactions 95 (1995) 41.
[4] J.S. Sieger, J. Non-Cryst. Solids 19 (1975) 213.
[5] M. Verità, F. Geotti-Bianchini, S. Hreglich, C.G. Pantano and V. Bojan, Bol. Soc. Esp. Ceram. Vid. 31C(6) (1992) 415.
[6] B. Yang, P.D. Townsend and S.A. Holgate, J. Phys. D: Appl. Phys. 27 (1994) 1757.
[7] H. Franz, Glastech. Ber. Glass Sci. Technol. 68 C1 (1995) 15.
[8] H. Doremus, Glass Science (Wiley, 1973).
[9] K.F.E. Williams, C.E. Johnson, J.A. Johnson, D. Holland and M.M. Karim, J. Phys.: Condens. Matter 7 (1995) 9485.

Physics of Thin Films

Advances in Research and Development

Edited by

GEORG HASS

Night Vision Laboratory
U. S. Army Electronics Command
Fort Belvoir, Virginia

and

RUDOLF E. THUN

Raytheon Company
Missile Systems Division
Bedford, Massachusetts

VOLUME 5

1969

ACADEMIC PRESS
NEW YORK AND LONDON

ACADEMIC PRESS, INC.
111 Fifth Avenue, New York, New York 10003

United Kingdom Edition published by
ACADEMIC PRESS, INC. (LONDON) LTD.
Berkeley Square House, London W1X 6BA

LIBRARY OF CONGRESS CATALOG CARD NUMBER: 63-16561

PRINTED IN THE UNITED STATES OF AMERICA

Numbers in pa

K. DEUTSCH

W. M. FEIST
sachusetts

M. H. FRA
Pennsylva

K. HIRSCHB

J. E. JOHN
Pennsylva

D. KOSSEL (

D. W. REA
Massachu

H. SCHROE
Germany

S. R. STEE
Massachu

ALFRED TH
fornia

Oxide Layers Deposited from Organic Solutions

H. SCHROEDER

Jenaer Glaswerk Schott & Genossen
Mainz, West Germany

I. Introduction

Methods to precipitate noble metals such as Ag, Au, and Cu from solutions onto solid substrates in highly reflecting layers have been known since the last century. It was only 30 years ago, however, that experiments to deposit dielectrics as liquid films onto nonmetallic substrates were initiated. The first studies of this kind were stimulated by Langmuir's observation (*1*) that certain insoluble substances of high molecular weight containing polar groups spread over a water surface as a monomolecular layer, and that such films could be deposited onto planar solid surfaces by slowly draining the water or raising the substrate. In 1935, Blodgett (*2*) produced antireflection coatings by this method, but did not pursue this approach any further since these coatings did not seem to offer any practical applications.

Soon thereafter, it was discovered in Germany that clear and stable SiO_2 films could be obtained by spreading colloidal solutions of silicic acid evenly over a glass surface, preferably by spinning the substrate. These studies

There is another fact which also supports the conclusion that organogenic oxide coatings, when deposited on glass as extremely thin layers (in case of TiO_2, $d \lesssim 50$ Å) are particularly free from stresses and flaws. Several observers have found that such layers normally show an even considerably increased hardness and abrasion resistance, as compared with layers of thicknesses in the order of $\lambda/4$. With these thin films an even higher abrasion resistance can be achieved than that shown by uncoated glass. This effect is therefore technologically used to improve the wear resistance of glass containers (*15*). The oxides most frequently used are TiO_2 or SnO_2. It is remarkable that the high resistance of extremely thin films can be obtained both by the cold-dipping process and by depositing finely dispersed fluid or evaporated compounds of the same materials on heated glass surfaces.

Although the existence of a tensile stress is particularly striking in coatings exhibiting a crystalline structure, it can be observed also in amorphous oxide layers having a low expansion coefficient compared with that of the substrate. In this case the stress is essentially of thermal origin. The normally small σ_i values, which have been found, for example, in SiO_2 coatings, can be enhanced, however, by adding to the solution soluble 'substances, which after baking of the coating are leached out in order to form a slightly porous layer. This method can be applied to create a controlled spherical bending of thin glass discs without the application of pressure.

IV. Special Oxide Layers

1. Titania

Of all high index materials, oxide layers obtained from titanium compounds have proved to be of especial practical interest. For this reason, titanium oxide coatings have been investigated with particular thoroughness. The results are, in some respects, also characteristic of the behavior of other coating materials suitable for the preparation of films by liquid coating processes. Therefore, they are treated here in more detail.

A surprising and perhaps specific property of TiO_2 films deposited from organic solutions is that their optical properties are dependent on the type of glass substrate. To understand this phenomenon an electron-optical study was made of the structures obtained with layers prepared from identical solutions on various glasses (*16*). The studies revealed that on alkali-free substrate the anatase structure is always formed (Fig. 8, sector A). However, if the glass substrates used contain sodium ions which can easily migrate (such as are present in window or plate glass), various types of "disturbed" TiO_2 structures may appear, the type depending on the rate of heating and to some degree on the initial compound. For example, layers deposited from

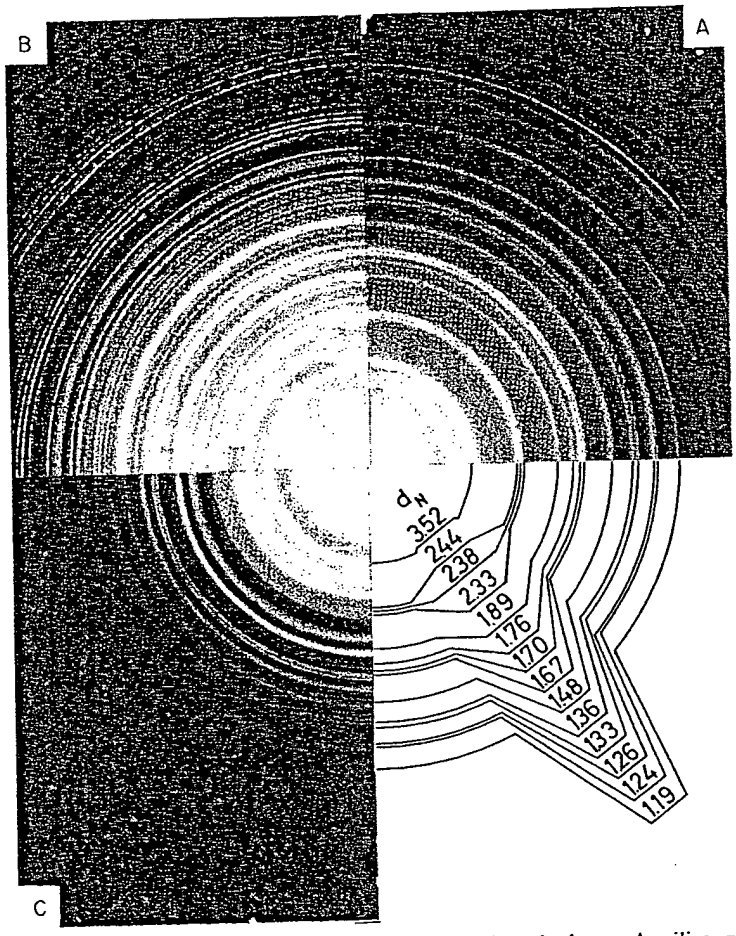

FIG. 8. Electron diffraction pattern of TiO_2 films deposited on: A, silica glass and rapidly or slowly heated; B, window glass and rapidly heated; C, window glass and slowly heated [d_N = spacings between the lattice planes (calculated from the radii of pattern a)].

a $TiCl_2(OC_2H_5)_2$ solution ("T_e films"), begin to form the brookite modification when heated rapidly (>25°C/min) to 450°C (Fig. 8, sector B). When, however, T_e films are heated slowly (<10°C/min), diffusion of Na^+ out of the glass surface leads to the formation of a crystal phase which exhibits the same diffraction pattern (Fig. 8, sector C) as the ones described in the literature (*17*) as Na_xTiO_2 or $Na_2O \cdot TiO_x \cdot TiO_2$. Since in our case no indication of the occurrence of a lower oxide of Ti in the solid films has been found, we choose to designate this phase here as "$Na_2O \cdot xTiO_2$." The electron micrographs of the three types of titania films, obtained by means of trans-

mission electron microscopy on samples separated from their substrates, are shown in Fig. 9. They reveal three completely different structures.

If a difficult to hydrolyze Ti compound, such as $Ti(OC_4H_9)_4$ ("T_b films"), is used instead of T_e, a structure of the type shown in Fig. 8c is always observed. In this case crystallization of TiO_2 is delayed so that sodium ions emigrating from the glass substrate are enriched sufficiently in the films to generate the $Na_2O \cdot xTiO_2$-type compound.

The strong influence of sodium ions present in the surface of a substrate on the film structure and composition of titania films can be demonstrated by the following experiment. A silica glass is covered on one side with powdered Na_2CO_3, heated up to 700°C for about 1 hr, and afterwards coated with a T_e or a T_b film. After baking, the coating exhibits the brookite or $Na_2O \cdot xTiO_2$ structure on the side pretreated with soda, and consists of anatase on the untreated side. On the other hand, the alkali influence was found not to be exerted by all types of glass containing sodium. On Schott glasses 2954 and 8405, for example, which contain between 7 and 8% Na_2O, TiO_2 coatings crystallize only in the anatase form. It may be concluded that in these glasses the diffusion velocity of the alkali ions is so small that it can not compete with the growth rate of the TiO_2 crystallites.

The films with different structures shown in Figs. 8 and 9 also exhibit marked differences in their optical properties. Figure 10 shows the spectral transmission curves of slowly heated T_e films deposited on both sides of (a) silica glass and (b) window glass. The well-known absorption of the latter has been eliminated in this graph by calculation. The evaluation reveals for the various types of films differences in the refractive index n and even more pronounced differences in the position of the uv-absorption edge*. In comparison with pure anatase type coatings, $Na_2O \cdot xTiO_2$ type films formed under slow heating conditions exhibit a lower n and a 14-nm shift of the absorption edge toward shorter wavelengths. On the other hand, brookite type coatings formed from T_e films at sufficiently high heating rates, have a uv cutoff wavelength which is almost identical with that of anatase layers. If T_b or other Ti compounds are used instead of T_e, the refractive index of the baked layers may deviate a little from those prepared from T_e films, since n depends on the packing density in each case. The uv absorption limit λ_s, however, is quite independent of the initial compound but depends on the specific crystal phase formed during baking.

The diffusion of sodium ions into and through a TiO_2 film proceeds rather fast even after the formation of crystals of a certain structure type in the film is terminated. This can be concluded from several observations. First,

* This edge is defined here by the intersection λ_s of the tangent at the point of inflection with the abscissa.

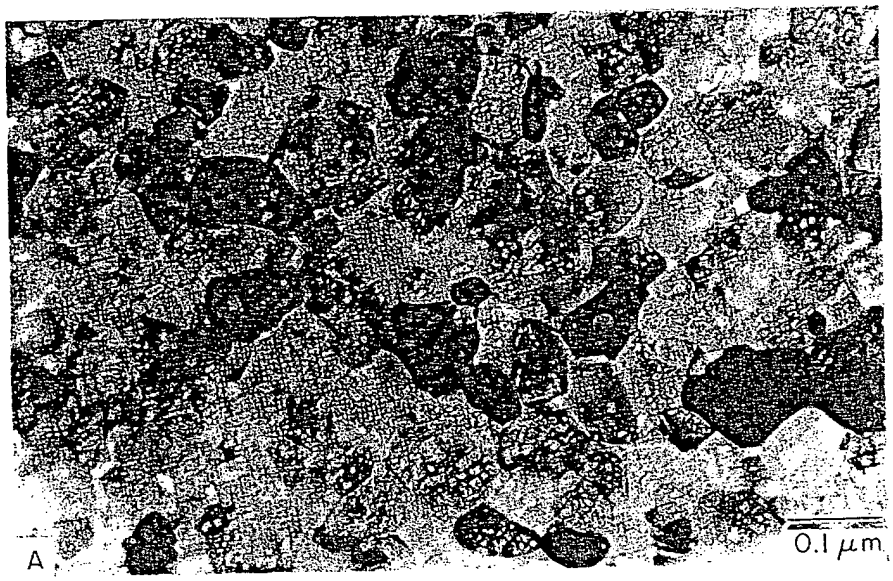

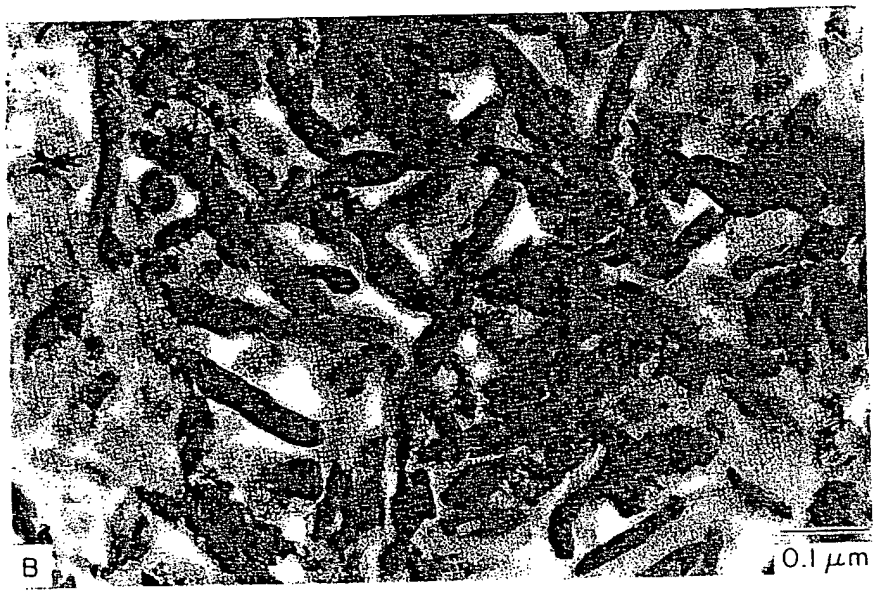

FIG. 9. Electron micrographs of the structures A, B, and C of Fig. 8.

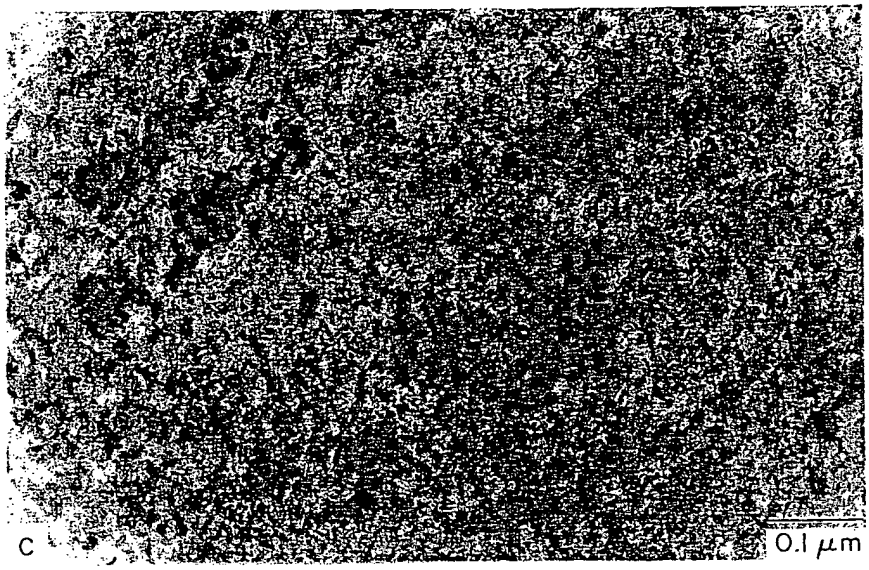

FIGURE 9c.

the "disturbed structures" can also be observed in diffraction patterns generated by electrons reflected at grazing incidence from the layers, unless their thickness is too large. In addition, after baking T_e films, tiny crystallites of NaCl are frequently detected on their surfaces. Remaining traces of Cl on the surface and sodium ions diffused through the film must be responsible for their formation. Finally, it has been found that baked TiO_2 films on soda-containing glasses do not form a substantial diffusion barrier against an ion exchange with silver immigrating from staining pastes at ~500°C. On the other hand, silica layers, produced in a similar way from solutions of silicic acid esters on glass, behave completely differently. They make an excellent diffusion barrier. A 200-Å-thick silica film is already sufficient to prevent, even at high temperatures most of alkali ions at the glass surface from migrating into a subsequently deposited TiO_2 film. Therefore the appearance of the various crystal phases in TiO_2 coatings on soda glasses can be controlled by means of a predeposited SiO_2 layer and by the heating rate. Figure 11 shows the result of deposition parameters on the uv absorption edge of titania films. A more detailed survey of the properties observed with T_e and T_b layers of $\lambda/4$ thickness, which were deposited on SiO_2 precoated window glass and heated up to 500°C, is given in Table I. This review shows clearly the competition between crystallization of TiO_2 in the anatase form and the Na^+ ions penetrating more or less rapidly into the films. If only small quantities of Na^+ have arrived before crystallization starts, the

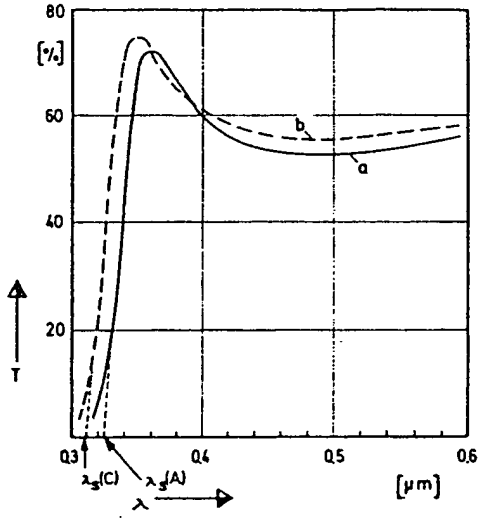

FIG. 10. Spectral transmittance of T_e films deposited on (a) silica glass, (b) window glass (both sides coated).

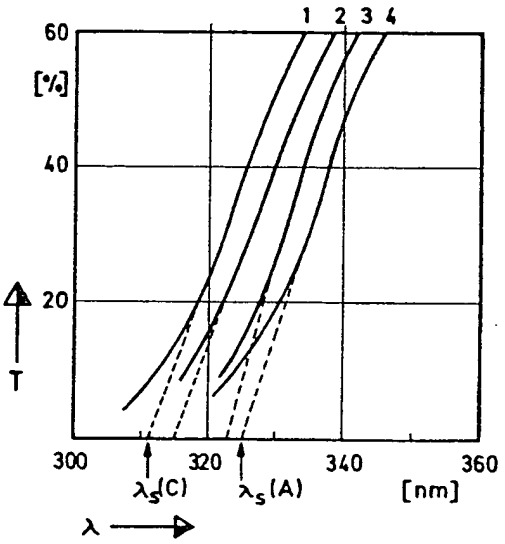

FIG. 11. Ultraviolet absorption edge of T_e films deposited on window glass precoated with SiO_2:

SiO_2 layer thickness d_s (nm)		0	6	12	18
Observed curve, when heated up	rapidly	3	3–4	4	4
	slowly	1	2	2–3	3–4

TABLE I

STRUCTURAL AND OPTICAL CHARACTERISTICS OF TiO_2 FILMS ($d \approx 60$ nm) ON WINDOW GLASS PRECOATED WITH SiO_2 FILMS OF VARIOUS THICKNESSES[a,b]

Thickness of SiO_2 film (nm)	TiO_2 from T_e soln, heated up		TiO_2 from T_b soln, heated up	
	50°/min	10°/min	50°/min	10°m/in
0	B (+C)[c]	C	C[d]	C (+A)
	323, 2.25	311, 2.24	315, 2.03	315, 2.03
6	B+A (+C)	C (+B)[d]	A (+C)	A+B
	324, —	315, —	323, —	323, —
12	A	B+C[d]	A	A (+C)
	325, 2.28	317, —	325, —	325, —
18	A	A+C	A	A
	325, 2.28	324, —	325, —	325, —
24	A	A	A	A
	325, 2.28	325, 2.28	325, 2.20	325, 2.20

[a] Crystal types: A, anatase; B, brookite; C, $Na_2O \cdot xTiO_2$.
[b] Numbers below indicate λ, (nm) and n measured for $\lambda = 550$ nm.
[c] Structure types in parentheses appear in minor quantities.
[d] Anatase appears in trace amounts only.

brookite type is induced, but as soon as higher quantities have passed over, the sodium is incorporated to form a $Na_2O \cdot xTiO_2$-type structure. In addition, the data listed in Table I allow a comparison of SiO_2 thickness values needed for the exclusion of $Na_2O \cdot xTiO_2$ crystals in T_e and T_b films.

It may be assumed that the emigration of alkali ions from glass substrates into freshly prepared solid films of titania is a phenomenon which might also occur with other film materials produced in a similar way. However, up to now, no publications describing such observations seem to exist.

In order to get further knowledge of the processes occurring during the solidification of titania films, the refractive index n (for $\lambda = 550$ nm) and the geometrical thickness d have been measured as a function of the baking temperature (ϑ_B) and the duration of the baking (t_B). T_e and T_b films of approximately the same thickness (~110 nm) were deposited on window glass, slowly heated up to ϑ_B, and tested after baking times of (a) 0.1, (b) 1, and (c) 10 hr. From the curves for T_e and T_b films shown in Fig. 12 it can be concluded immediately that for T_e the formation of the oxide layer is substantially terminated at a rather low temperature of about 250°C. This results obviously from the fact that the hydrolytic reaction of the liquid film with air moisture starts at room temperature and is already finished after moderate heating. With T_b, however, which is much more resistant

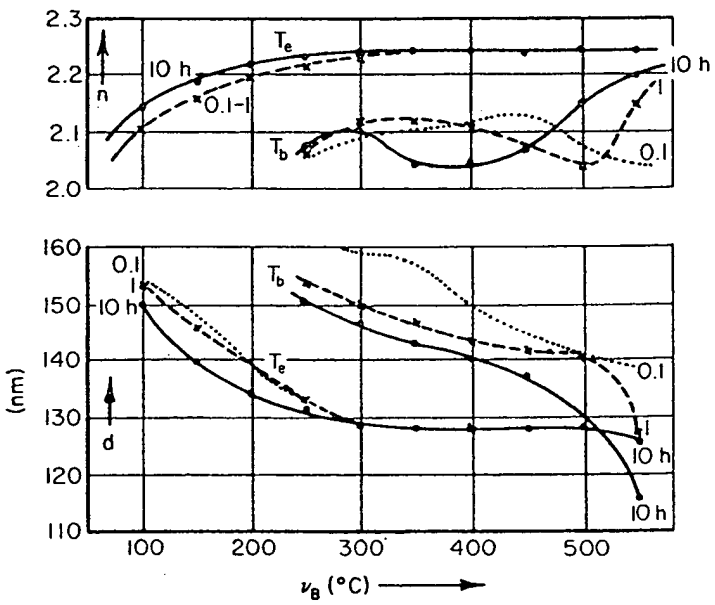

FIG. 12. Refractive index n ($\lambda = 550$ nm) and thickness d vs baking temperature ϑ_B for T_e and T_b films (parameter, baking time t_B).

to hydrolysis, the transformation phenomena produced essentially by pyrolysis extend over the whole temperature rise up to the softening range of the glass. It can further be seen that the n curve, which first rises to a maximum, then drops to a minimum, before showing again a considerable rise, shifts toward a lower temperature when t_B is increased. This means that n can be expressed by a function of the form

$$n = F(\vartheta_B f(t_B)).$$

The d curves of T_b films show a similar displacement of values toward lower temperatures when the baking time is increased from 0.1 to 10 hr.

This behavior can be interpreted as follows. During the first rise of n after the evaporation of the solvent, the T_b film becomes more compact without substantial loss of its mass. At this stage the first crystal nuclei have already formed. When $u = \vartheta_B f(t_B)$ exceeds a certain amount, the organic decomposition products and eventually H_2O, which have been formed during the pyrolysis, are gradually expelled so that despite a further decrease in thickness, the density, and thus also the refractive index both diminish. When u increases further, the porous assemblage of crystallites, consisting in the case under consideration of $Na_2O \cdot xTiO_2$, starts to condense. This

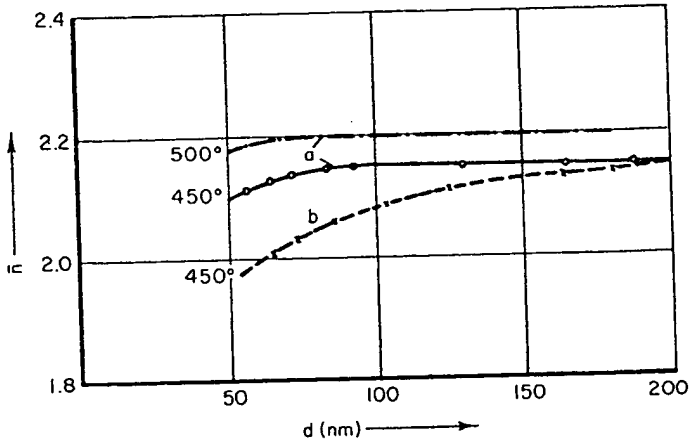

FIG. 13. Mean refractive index $\bar{n}$ ($\lambda = 500$ nm) as a function of layer thickness of T_b films deposited on (a) silica, (b) window glass.

leads to a rise of n to a value which the T_e films have already attained at 250°C, and to a still further decrease of d. It is, however, remarkable that the refractive indices attained are still considerably lower than those of compact titania crystals, so that despite the high degree of hardness of the layers, the volume factor computed from the molar refraction hardly exceeds 0.90.

On the other hand, higher indices can be attained in titania layers if certain heavy metals such as bismuth or lead are incorporated as oxides, and if the influence of alkali is sufficiently suppressed. Under these conditions the increase in refractive index is accompanied by a shift of the uv absorption limit toward longer wavelengths.

An attempt was made to investigate the structure of T_e films containing an admixture of $BiCl_3$ (31 g Bi_2O_3:100 g TiO_2). If the films are deposited on silica glass and fired at temperatures up to ~500°C, the only crystal type observed is anatase. After treatment at higher temperatures, however, the diffraction pattern also reveals the formation of rutile crystallites. This transformation into rutile goes to completion at a temperature of 600–700°C if the silica substrate has been precoated with a SiO_2 film of approx $\lambda/4$ thickness prepared from a silicic acid ester solution. In the case of a precoated window glass this transformation is accomplished only above 850°C, whereas at lower temperatures increasingly higher portions of anatase and $Na_2O \cdot xTiO_2$ are formed. From these observations it can be concluded, first, that the minimum thickness of the diffusion inhibiting SiO_2 layer increases with a higher content of Cl^- ions, and second, that the anatase lattice is stabilized by sodium ions penetrating into the T_{e+Bi} film. The refractive indices n

obtained in such films on silica substrates range from 2.30 to about 2.50 for $\lambda = 550$ nm, depending on the firing temperature and period.

Since the process of alkali emigration from a substrate into a crystallizing film requires a certain time, the influence on the resulting structure type can be expected to decrease more or less from the substrate–film boundary to the film–air boundary, depending on film thickness d. Consequently, since the refractive index of $Na_2O \cdot xTiO_2$-type films was found to be considerably lower than that of anatase-type ones, thin layers deposited on alkali glasses should exhibit lower mean indices $\bar{n}$ than thicker ones. Figure 13 shows the results of measurements of $\bar{n}$ at $\lambda = 500$ nm obtained with T_b films deposited (a) on silica glass and (b) on window glass, both baked 1 hr at 450°C and 500°C, respectively. In the case (a) only a slight drop of $\bar{n}$ occurs at film thicknesses of less than ~80 nm, which may be caused by a decreasing packing density near the substrate due to a restriction in the sintering possibility. On window glass (b), however, the alkali diffusion into the T_b films leads to a Na-concentration profile which obviously falls down rapidly at a distance of about 50 nm from the substrate, so that the mean refractive index increases continuously if the film becomes thicker than 50 nm. According to the theory of light reflection at inhomogeneous layers (*18*), it is possible to determine n_a and n_s, the values of n at the film–air and the film–substrate boundaries, from the reflectance values at maximum and minimum. Actually, such measurements carried out for rather thick T_b films on window glass yielded for $\Delta n = n_a - n_s$ values up to $\simeq 0.15$.

Since the refractive index n of TiO_2 layers produced from organic solutions is dependent on a series of parameters during their formation, it is evident that the dispersion, n_λ must likewise exhibit corresponding variations. However, if a reduced dispersion N_λ is introduced by relating the n_λ values of each individual curve to those at $\lambda = 550$ nm, i.e., $N_\lambda = n_\lambda / n_{550}$, all curves for N_λ become nearly identical, no matter which Ti compound, concentration, or substrate has been used and which crystal type appears (see Fig. 14). In addition, this curve coincides largely also with that calculated from dispersion data for bulk TiO_2 (*19*). Deviations from this function N_λ which is characteristic for TiO_2, become noticeable only if oxides are incorporated which have markedly different absorption properties in the uv or visible region, or when suboxides have been formed in the presence of reducing ingredients.

For certain T_b coatings with anatase structure, applied on fused quartz, the optical constants n and k were also determined in the short-wavelength absorption region. The thickness d was first determined from the spectral position of the reflectance maxima and minima in the region where $k = 0$ ($\lambda > 420$ nm). Thereafter were evaluated n_λ and k_λ from measurements of T_λ and R_λ in the region of $\lambda = 200$–1000 nm, using a calculation method

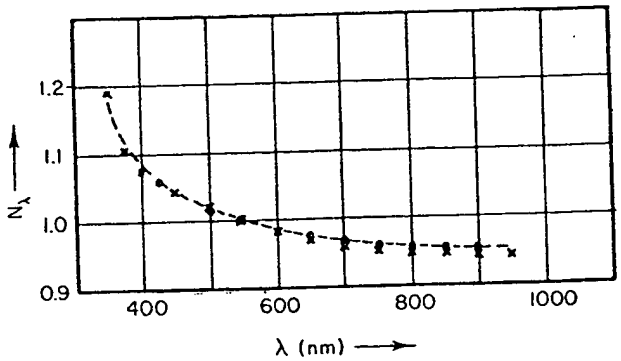

FIG. 14. Reduced dispersion N_λ of various TiO_2 materials in the visible region: (×) films with anatase structure; (●) films with C-type structure; (- - -) bulk material (anatase, mean values over the crystallographic axes).

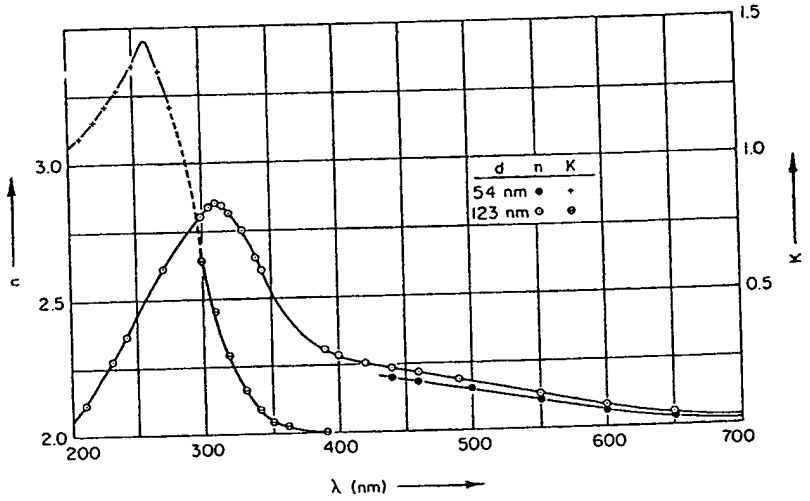

FIG. 15. Optical constants n, k of T_b films ($d = 54$ and 123 nm) on silica glass, calculated from measurements of T_λ and R_λ ($\vartheta_B = 430°C$).

applying to homogeneous layers. The results are recorded in Fig. 15 for two layers of $d = 54$ and 123 nm, respectively. They reveal again a slight dependence on d of the n values as exhibited in Fig. 13.

2. SILICA

SiO_2 has gained its importance for practical applications of the cold-dipping method by the fact that it is the only substance with which hard and stable layers with a refractive index <1.5 can be obtained. Numerous suggestions for the preparation of SiO_2 films are published in the patent